



# Optimizing classroom modularity and combinations to enhance daylighting performance and outdoor platform through ANN acceleration in the post-epidemic era

Yubo Liu<sup>\*</sup>, Kaifan Chen, Eryu Ni, Qiaoming Deng

School of Architecture, State Key Laboratory of Subtropical Building Science, South China University of Technology, Guangzhou, 510640, Guangdong, China

## ARTICLE INFO

### Keywords:

Primary and secondary school classrooms  
Daylighting  
Post-epidemic era  
Artificial neural network  
Multi-objective optimization

## ABSTRACT

The global COVID-19 pandemic has increased attention to the relationship between the built environment and health, particularly in educational settings where students spend a significant amount of their time. Traditional side daylighting used in schools, while cost-effective and easy to construct, can result in uneven indoor daylighting. To address this issue, this paper proposes a terraced teaching building design model for primary and secondary schools in Guangzhou based on the design experience of an “open-air school movement” during a historical respiratory epidemic in the early 20th century. The proposed design relies on skylight for lighting, and each classroom has an outdoor platform. An optimization algorithm based on Spatial Daylight Autonomy (sDA), Uniformity of Daylighting (UOD), Annual Sunlight Exposure (ASE), Outdoor Platform Area (OPA), Gable Wall Length (GWL), and Space Utilization (SU) is used to obtain the optimal concrete form of the building. To speed up the simulation process, a set of Artificial Neural Network (ANN) based rapid prediction network models for complex forms is proposed. This group prediction method improves the simulation speed by 357 times and grossly speed up the optimization process based on six indexes in the early design stage, resulting in four terraced teaching buildings that meet the above criteria. Overall, the proposed design provides a novel architectural form that ensures overall visual comfort while promoting students’ learning and physical health.

## 1. Introduction

### 1.1. Background

As the global pandemic gradually subsides and comes under control, society and the economy recover from this sudden event, individuals are now shifting their focus towards the aftermath of the pandemic and specifically contemplating the design of classroom spaces in primary and secondary schools from a health standpoint. Central Europe’s population spends approximately 80–90% of their time indoors [1,2] while a study conducted in the United States revealed that children and adolescents primarily reside indoors, within the confines of classrooms [3]. However, students who spend prolonged periods indoors often face limited exposure to natural

<sup>\*</sup> Corresponding author.

E-mail address: [liyubo@scut.edu.cn](mailto:liyubo@scut.edu.cn) (Y. Liu).

<https://doi.org/10.1016/j.heliyon.2023.e21598>

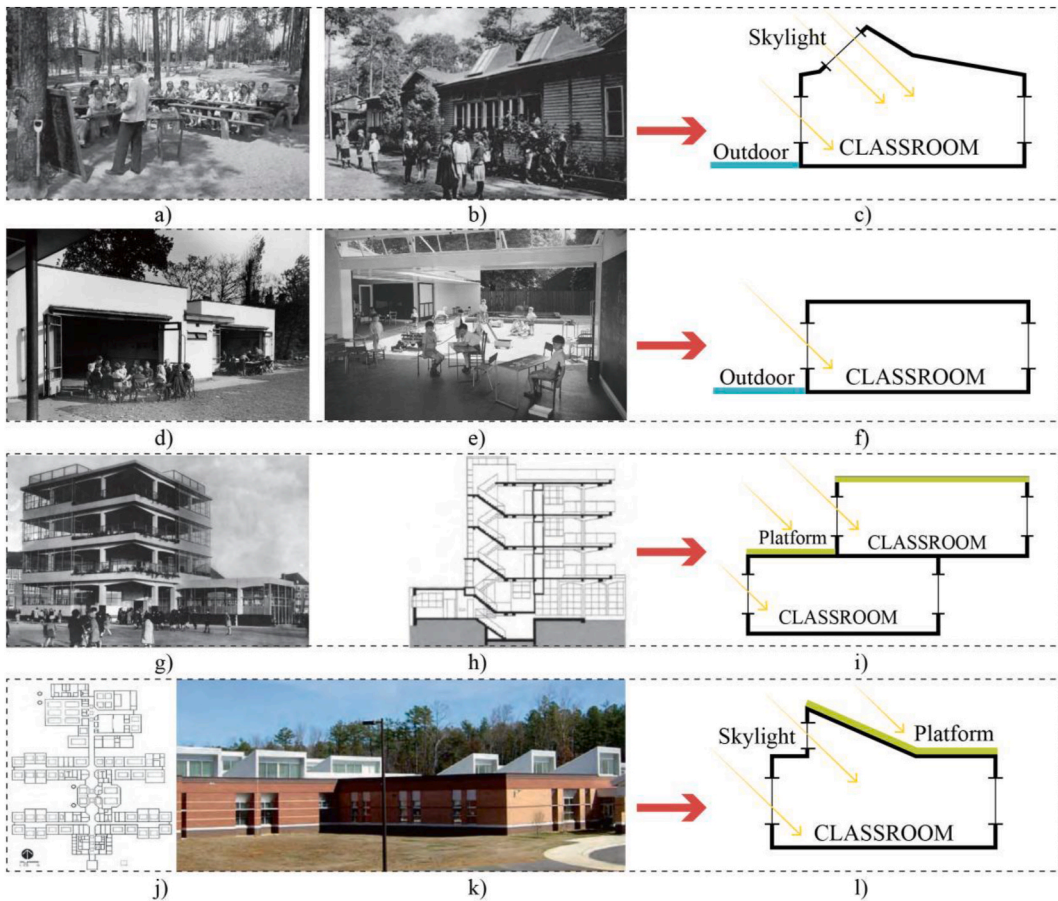
Received 31 May 2023; Received in revised form 29 September 2023; Accepted 24 October 2023

Available online 2 November 2023

2405-8440/© 2023 The Authors. Published by Elsevier Ltd. This is an open access article under the CC BY-NC-ND license (<http://creativecommons.org/licenses/by-nc-nd/4.0/>).

daylight. As urban areas expand and become denser, the lack of effective design strategies further diminishes their access to daylight. Consequently, various health issues arise. For instance, the global rise in myopia since the 1960s has been linked to reduced sunlight exposure, and inadequate exposure to sunlight can result in diverse bone and psychological disorders [4]. Research [5–7] has demonstrated that natural light significantly influences hormone secretion in primary and secondary school students, which plays a vital role in promoting their healthy growth and enhancing learning efficiency—an effect that cannot be replicated by artificial lighting. Hence, the presence of a natural light environment in classrooms is crucial for students in this critical period of growth and development. Unfortunately, in China, these problems are exacerbated by the immense population density and rapid urbanization witnessed in the past two decades. According to the World Health Organization’s 2019 World Vision Report, China possesses the highest youth myopia rate globally. This is primarily attributed to the uneven distribution of natural light in traditional side-windowed classrooms, where lighting near the windows is excessively intense for reading, while the area further away remains inadequately lit. Such abrupt variations in illumination can cause significant visual discomfort and eye fatigue as students shift their gaze within the classroom [8], leading to other health issues [9]. Consequently, it has become common practice for curtains to be drawn and artificial lights to be used during the day in primary and secondary school classrooms in China. Consequently, young individuals are deprived of exposure to sunlight within the classroom. This deprivation can negatively impact students’ learning and health, as well as significantly impair their immunity [10]. Hence, it is of utmost importance to design classrooms that rely solely on natural light rather than artificial lighting.

Traditional design practices commonly employ “post-evaluation” as a means to validate the design’s accuracy [11]. However, this approach has evident limitations. Real-time feedback on lighting indicators cannot be obtained during the design phase, and there is a lack of comprehensive control over the building’s form and lighting performance in the early stages of design, leading to delayed issue identification. It has been proven that making modifications in the later stages of design or even after the building’s completion is expensive and yields minimal benefits [12]. To overcome these challenges, many researchers have developed performance simulation tools such as Ladybug Tools to aid in optimizing building design. However, the simulation speed provided by external engines is still limited in delivering real-time previews of lighting performance during the early design stages. Recent advancements in deep learning technology have led some scholars to focus on data-driven performance evaluation [13]. By pre-training a substantial amount of



**Fig. 1.** The early open-air school. a-b: Charlottenburg Forest School. d-e: King Alfred School. g-h: Open Air School in Amsterdam. j-k: Smith Middle School (Picture a-b, g-h from the Internet; picture d-e from INNER-LONDON SCHOOLS; picture j-k from Ref. [20]).

sample data and fitting it into a functional model, rapid performance predictions can be achieved. This approach enables designers to shift away from relying solely on “post-evaluation” models, thereby enhancing their ability to predict and control the final design outcome.

### 1.2. Learning from history

To examine classroom models that rely on natural lighting in the post-epidemic era, this paper draws inspiration from historical examples. Over a century ago, European countries commenced experiments with different classroom designs in response to tuberculosis and the Spanish flu outbreaks. These models, referred to as the “open air school movement,” were developed during that period, and certain instances of their usage continue to exist today. As artificial lighting options similar to electric lights were unavailable during that period, architects of the time maximized natural light by incorporating large windows on the sides and ceiling of each room. Furthermore, outdoor areas matching the size of the classrooms allowed for open-air teaching, which increased sunlight exposure and enhanced student immunity [14]. Constructed in 1904, the Charlottenburg Forest School in Germany (Fig. 1a and b) pioneered the concept of open-air schools by incorporating extensive glass windows and skylights to enhance indoor lighting [15]. Flexible furniture allowed students and teachers to move outside the classrooms to take advantage of optimal natural lighting when weather conditions allowed [16]. The Charlottenburg Forest School gained widespread recognition for its high recovery rate and improvements in student health. Likewise, the Junior school classrooms at King Alfred School in the UK (Fig. 1d and e) and the Open Air School in Amsterdam, the Netherlands (Fig. 1g and h), achieved significant success. It is noteworthy that the majority of open-air schools were single-story buildings customized to meet specific requirements, with the Amsterdam Open Air School being a rare multi-story example designed to maintain a connection between indoor and outdoor spaces. However, its open-air classrooms, featuring large balconies, had significantly lower natural lighting compared to single-story classrooms and fully outdoor spaces. In the United States, numerous open-air schools were built in California and New York, and there were even proposals for all primary and secondary schools to embrace the open-air school model in the future. However, following the war, with economic and energy advancements, “open-air schools” gradually disappeared and were substituted by “windowless classrooms” equipped with artificial lighting [17]. In 1975, facing mounting student misbehavior, boredom, and teacher frustration stemming from the absence of natural light [18,19], the model was abruptly terminated despite resistance. Attention subsequently returned to classroom designs that prioritize the incorporation of natural daylight (Fig. 1j and k).

Starting from 1980, multiple publications in Europe and the United States advocated for the incorporation of natural light in classrooms. An example of such a publication is the “Guide for Daylighting Schools” issued by the Lighting Research Center (LRC), which highlights the importance of natural light and recommends that students receive at least two-thirds of their classroom time under its illumination [21]. Another significant resource is the British BUILDING BULLETIN90-Lighting Design for Schools, which emphasizes the importance of natural lighting in primary and secondary school classrooms. It advises utilizing natural light under normal weather conditions and resorting to artificial lighting only in severe weather conditions [22]. Drawing inspiration from this philosophy, Alan Ford’s projects in Australia and Innovative Design in the United States have emerged as exemplary models for classrooms with natural lighting [23–26]. An outstanding illustration is Smith Middle School in Calboro, North Carolina, USA, which implemented a north-facing vertical skylight on its roof to optimize the intake of natural light. These explorations have resulted in innovative school building designs that differ from conventional side window lighting.

### 1.3. Research aim

The COVID-19 pandemic, regarded as the most severe global epidemic since the Spanish influenza outbreak in the previous century [27], underscores the importance of “open-air schools” in designing classrooms with ample daylighting in the post-pandemic era. This study synthesizes historical classroom design experiences from Europe and the United States, extracting four design elements (Fig. 1: c, f, i, l). The proposed model incorporates these elements and introduces top daylighting as an additional lighting method for all types of classrooms. Top daylighting, which offers more uniform daylighting compared to side daylighting [28–31], has been demonstrated to enhance students’ exam performance [32]. Moreover, ANSI/ASHRAE/IES Standard 100-2018 promotes the use of skylight lighting to reduce building energy consumption [33]. However, achieving classrooms with skylight lighting in conventional multi-story buildings and providing large outdoor activity spaces, as historically advocated, pose significant challenges due to the characteristics of skylights and the current trend of high density in Chinese cities. Therefore, the aim of this paper is to propose a terraced classroom layout that addresses these challenges. By incorporating setbacks in the building design, skylights protruding from the roof can be utilized, ensuring a more uniform distribution of natural light within the classrooms. Additionally, the exposed gable walls of each classroom enhance indoor daylighting and ventilation by integrating tall side windows. Moreover, these large side windows can be connected to the exterior roof deck, which not only enhances indoor daylighting performance but also provides a platform for students to conduct classes and participate in outdoor activities when weather permits. This idea is also presented by Spennemann et al. [27] in the design of post-epidemic schools. Furthermore, to tackle the challenge of achieving a harmonious balance between daylighting performance and aesthetics in the early design stage, this study utilizes deep learning to provide real-time predictions of Spatial Daylight Autonomy (sDA), Annual Light Exposure (ASE), and Daylighting Uniformity (UDI). Subsequently, the Outdoor Platform Area (OPA), Gable Wall Length (GWL), and Space Utilization (SU) are integrated as comprehensive control and evaluation metrics in the Wallacei plug-in, allowing for efficient optimization of form and daylighting performance in the early design stage.

The paper is structured as follows: Section 2 offers a literature review on optimizing classrooms through daylighting performance and investigates the use of deep learning to enhance daylighting performance. Section 3 outlines the entire experimental workflow,

which includes constructing parametric prototypes, defining classroom combinatorial rules, preparing the dataset, training the artificial neural network (ANN), and conducting multi-objective optimization. Section 4 presents the results of ANN training and multi-objective optimization. Section 5 discusses the entire experimental process and its outcomes. Finally, Section 6 summarizes the key conclusions of the paper.

## 2. Literature review

### 2.1. Classrooms optimizing based on daylighting performance

With the increasing focus on natural light in indoor environments, numerous researchers have been conducting investigations in this area. Certain scholars focus on improving natural lighting conditions in educational environments by considering factors such as thermal comfort and energy efficiency. For example, Khaoula et al. [34] enhanced the performance of primary and secondary school classrooms in hot-dry regions by evaluating parameters such as window-to-wall ratio, shading, and glass type. They suggested that a balance between daylighting and thermal comfort can be achieved by increasing the window area, utilizing fixed shading devices, and using high-quality glass. Bakmohammad et al. [35] improved daylighting performance and reduced energy consumption by analyzing the impact of parameters such as classroom orientation and window shape on both daylighting and energy usage. Zhang et al. [36] integrated multiple design parameters, such as room depth, corridor depth, window-to-wall ratio, and glass material, to optimize both daylighting and thermal performance in school buildings situated in the cold climates of northern China.

Moreover, ensuring uniform indoor daylighting is crucial for avoiding visual discomfort caused by excessive brightness or inadequate daylighting in specific areas of the space. Callejas et al. [37] led a research project that investigated the enhancement of natural light levels in prefabricated modular classrooms in Chile. The study findings showed that by combining top horizontal skylights and vertical reflective elements, the distribution of daylight within the classroom could be optimized for uniformity. Salomón et al. [38] conducted a study that observed a modest improvement in interior uniformity through the inclusion of reflectors on the side windows. Additionally, they suggested the use of roller-type curtains with sunscreen fabrics as an additional measure to further enhance interior uniformity. Likewise, Zhu et al. [39] optimized the uniformity of indoor lighting in kindergartens situated in five different climate zones in China.

However, the research in the mentioned studies are focused on individual classrooms within a single setting, disregarding the influence of shading and light reflection from the surrounding environment in real-life scenarios. This oversight can result in significant disparities between optimization outcomes and actual application conditions. Moreover, within the present-day densely inhabited urban environments across the globe, classrooms frequently showcase recurring arrangements, both in terms of their horizontal and vertical configurations, regarding their overall structure and cross-sectional design. As a consequence, there is a prevalence of classrooms with side daylighting and a lack of top daylighting options that offer superior illumination effects. Consequently, there exists a scarcity of research investigating various arrangements of classrooms, both vertically and horizontally. In this particular study segment, Liu et al. [40] conducted optimization of a two-story school building by recessing the upper-level classrooms, enabling skylight illumination in each classroom and enhancing the overall natural lighting. However, their study exclusively examines the classroom section of a two-story case, neglecting the exploration of the entire building involving multiple levels. This paper aims to address this gap. Additionally, Wang et al. [41] proposed a framework for form optimization that integrates natural lighting and topology principles. By selectively removing different components from a predefined volume, they generated diverse building volumes that met the criteria for natural lighting while showcasing significant topological variations. Similarly, Wang et al. [42] presented a workflow that combines performance considerations to optimize a range of building forms. However, it is important to note that the latter two studies were not exclusively tailored to primary and secondary school classroom combinations; rather, they provided a general framework for performance-driven optimization of building volumes across multiple building types, which can provide insights for optimizing the arrangement of numerous classrooms.

Although these studies yield valuable results, the optimization process often requires significant time investment.

Usually, it requires a span of 3–5 days or even longer to optimize various performance indicators of multiple solution set. If there are issues with parameter settings or unsatisfactory optimization results, researchers must start the entire experiment process from scratch, leading to considerable time expenditure. Hence, there is a need for new technologies to expedite the optimization process and reduce time costs.

### 2.2. Optimizing with deep learning acceleration

With the growing popularity of artificial intelligence (AI) computing methods, Deep Learning (DL) algorithms have matured and are being utilized by researchers for efficient prediction and optimization of building performance, addressing the time-consuming nature of traditional methods [43–45]. To compare the accuracy of different algorithms, researchers have conducted evaluations. For instance, Arbab et al. [46] compared the performance of RF, DT, support vector regression (SVR), and neural network models in predicting daylighting and energy performance of office spaces in Tehran, Iran. The results demonstrated that artificial neural networks provided higher prediction accuracy. Among the 25 studies reviewed by Ngarambe et al. [47], 22 employed supervised neural network algorithms for daylight optimization, while the remaining 3 used multiple linear regression or density-based clustering algorithm (DBSCAN). Artificial neural networks currently stand out as the preferred algorithm for accelerating and optimizing daylighting within the realm of deep learning algorithms. For example, Han et al. [48] developed an ANN-based daylighting prediction model for a single rectangular office unit, incorporating parameters such as wall thickness, material reflection ratio, and window sill



height. The model achieved an R2 value of 0.988 and 0.996, ensuring accuracy and boosting prediction speed by 250 times compared to traditional methods. Lin et al. [49] proposed a neural network model based on intermediary features using sDA and ASE, enabling the prediction of daylighting performance in architectural curtain wall design and offering a tool for architects and designers to rapidly evaluate and compare different design schemes. Moreover, Luanet al. [50] explored daylighting prediction using various layouts with single-layer plane shapes, thereby expanding the application range of ANN-based daylighting prediction. Thus, with the aid of DL technology, a relatively mature workflow has been established, encompassing real-time prediction and multi-objective optimization. Many scholars have adopted this workflow in their research. For example, Xu et al. [51] trained a neural network based on lighting, heat, and energy consumption in classrooms, utilizing the output for optimization objectives to guide the design of primary and secondary school classrooms in southern China. Wanget al. [52] discussed a design framework based on performance optimization and prediction, specifically applicable to the schematic design of primary and secondary school teaching buildings. A similar approach was taken by Yukai Zou [53] et al., who defined more detailed design parameters for classrooms with side-window lighting.

In this investigation, ANN will be employed to forecast various daylighting metrics while considering the influence of the surrounding environmental factors. The developed model will be incorporated within a multi-objective optimization framework, aiming to expedite the optimization procedure based on the performance of light harvesting.

### 3. Research method

#### 3.1. Workflow

This study primarily employs Grasshopper to conduct modeling and simulation while integrating external Python libraries to facilitate optimization. The experimental procedure entails three stages, as illustrated in Fig. 2: the creation of training data, training and testing of an ANN model, and multi-objective optimization using a genetic algorithm. The initial stage concentrates on generating and constructing terraced classroom combinations for the study, while the latter two phases primarily address enhancing work efficiency and optimization methods.

Nomenclature		HCS	Height of Classroom with Skylight
sDa	Spatial Daylight Autonomy	HCSW	Height of Classroom with side-window
UOD	Uniformity of Daylighting	RD	Room Depth of Classroom
ASE	Annual Light Exposure	RW	Room Width of Classroom
OPA	Outdoor Platform Area	BH	Beam Height
GWL	Gable Wall Length	RW	Reflectance of the Wall Surface
SU	Space Utilization	RG	Reflectance of the Ground Surface
FN	Floor Number	RR	Reflectance of the Ground Roof
DSA	Displacement of the Skylight Apex	RS	Reflectance of the Shade Surface
DS	Displacement of the Skylight	TW	Transmissivity of Window
ESC	Extent of skylight coverage	WT	Wall Thickness
SKH	Skylight Height	WC	Width of Corridor
SH	Sill height	ANN	Artificial Neural Network
FW	Length of the front wall on north face	DF	Daylight Factor
		RW	Length of the rear wall on north face

#### 3.2. Parametric classroom modeling

Parameterized design, initially defined as “parameter-based dimensional relationship” by Moretti [29] and later expanded upon by Kalay, enables the real-time visualization of geometric relationships in a parameterized model as the parameters change [30]. In this paper, in order to explore the optimal parameters combination, a parametric model is constructed in the initial step.

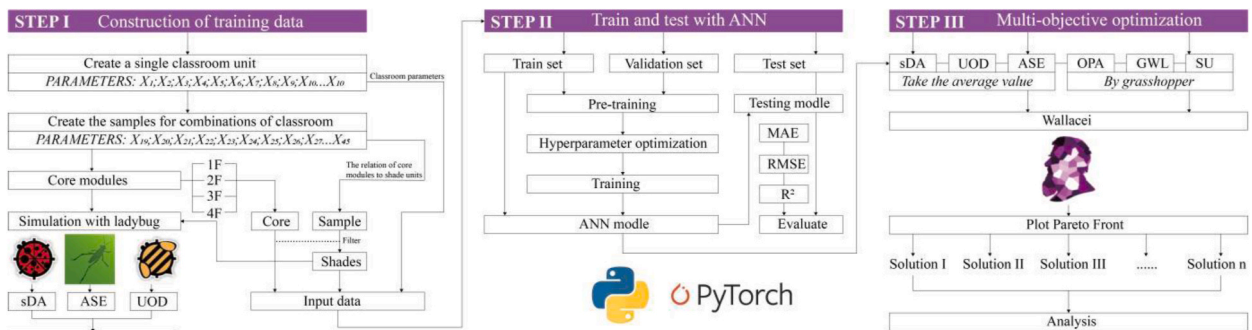


Fig. 2. Workflow diagram.

The selected climate setting for this study is situated in the Guangzhou region of China. To mitigate the impact of heat radiation within the room, the primary orientation of the classroom was aligned towards the north direction, and a single corridor on the south side is adopted as the corridor type. A rectangular plane serves as the bottom plane of the classroom unit, while the north and south sides and the top are used as the primary daylighting surfaces. The form of top daylighting refers to existing relevant practice research [20,54,55] and the experience from the history mentioned above, and various types of top daylighting forms are included in a parameter system that controls Skylight Height (SKH), Displacement of the Skylight (DS), Displacement of the Skylight Apex (DSA), and other parameters. In terms of parameter selection and control for classroom design, the Room Depth (RD) and Room Width (RW) serve as crucial parameters for improving the model's adaptability. These parameters must adhere to the specifications outlined in China's "Design Code for Primary and Secondary Schools" (GB50099-2011) [56] to ensure compliance. Specifically, the average area per middle school student is 1.39 square meters according to GB50099-2011. Considering a classroom with 45 students, the minimum room area calculated using the RD and RW is 63 m<sup>2</sup>. In addition, to prevent blackboard glare, the GB50099-2011 mandates that the headwall's width of side window at the front of the classroom must not be less than 1 m. Thus, for this experiment, the front headwall is set at 1.2 m, while the rear headwall is set at 1 m. To ensure the optimal indoor daylight environment, the tops of the north-side windows and south-side window extend from the upper part of the sill to the bottom of the beam, and the beam height is uniformly set at 700 mm. The width of the south-side window is uniformly offset by 1.8 m from the classroom width to allow for two main entrances. Based on these criteria, other main control parameters are displayed in Table 1. This paper introduces two parametric classroom model shown in Fig. 3: Parametric model I (Fig. 3-a), which incorporates parameters related to top daylighting, part of the classrooms generated with the change of parameters is shown in Fig. 4a-l, and Parametric model II (Fig. 3-b), which focuses on parameters associated exclusively with side daylighting.

Throughout the process of constructing the dataset and subsequently training, the parameter configurations for both skylight daylighting and side daylighting classrooms in a single sample are unique. This is intended to mitigate the impact of varying parameters of classroom on daylighting effects, while also reducing the computational load of the model and enhancing its predictive accuracy.

### 3.3. Combination rules

#### 3.3.1. Reserve roof area

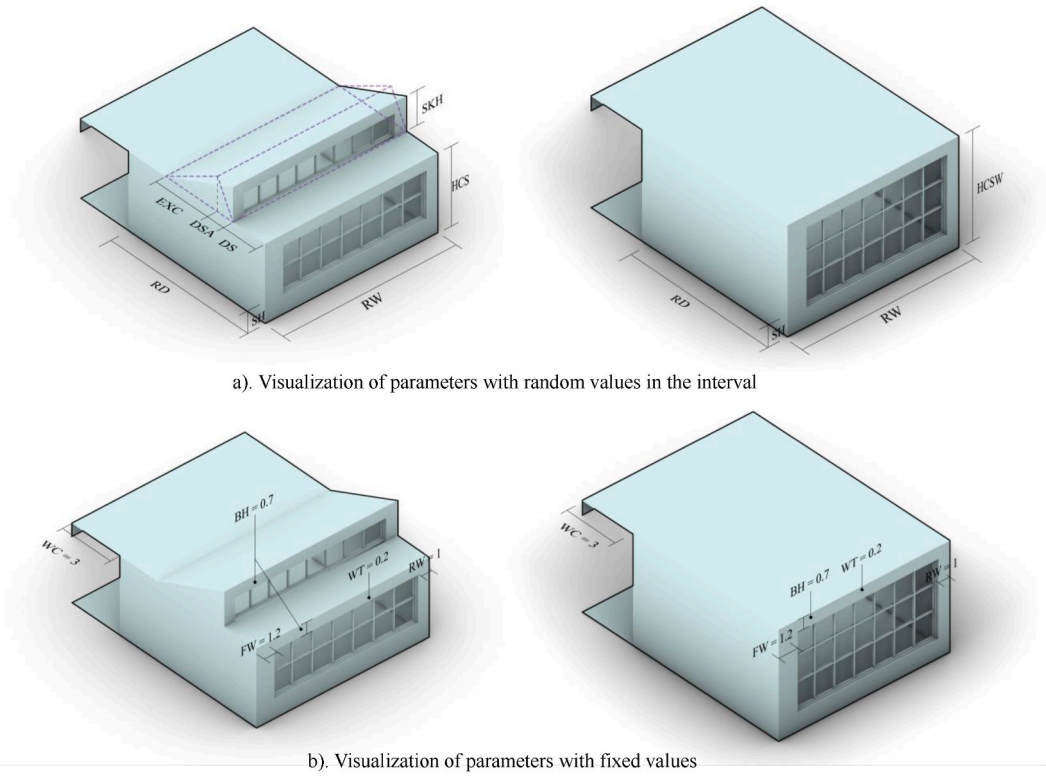
As depicted in Fig. 5a-c, in order to optimize top daylighting for each classroom, those located above the first floor have been systematically moved towards the southern direction, thereby allowing for the full allocation of roof space per classroom floor. This approach not only ensures optimal daylighting for lower-level classrooms but also provides an outdoor activity space for same-level classrooms.

#### 3.3.2. The three-story classroom increases the story height

In accordance with the GB50099-2011 [56] of China, the classrooms of primary and secondary school are generally limited to a maximum of four floors. However, a terraced with four stories would grossly increase the depth of the building, which could be less more conducive to the layout of the building on the site. Based on prior research on the correlation between classroom height and daylighting [57], it has been observed that side-windows play a progressively more significant role in illuminating indoor spaces as the height of the classroom increases. Conversely, in classrooms equipped with skylights, the contribution of skylights to indoor daylighting performance diminishes as the height of the room increases. For classrooms with side daylighting, the floor height of at least 4.5 m is recommended to apply. Therefore, the parametric model II is used in third floor, or rather this paper cancel the three-story's setback to reduce depth and improve SU, and instead increase the classroom floor height to compensate for the lack of

**Table 1**  
Values and intervals of design variables.

Input	Range	Step	Unit	Explanation
FN	1-4	1	/	Floor Number
DSA	0-5	0.1	m	Displacement of the Skylight Apex
DS	0-4.2	0.1	m	Displacement of the Skylight
EXC	2-4.6	0.1	m	Extent of skylight coverage
SKH	1.2-2.5	0.1	m	Skylight Height
SH	0.5-1.5	0.1	m	Sill height
HCS	3.6-4.6	0.1	m	Height of Classroom with Skylight
HCSW	4.6-6	0.1	m	Height of Classroom with side-window
RD	7-9.5	0.1	m	Room Depth of Classroom
RW	7-10	0.1	m	Room Width of Classroom
BH	0.6	/	m	Beam Height
RW	0.8	/	/	Reflectance of the Wall Surface
RG	0.4	/	/	Reflectance of the Ground Surface
RR	0.8	/	/	Reflectance of the Ground Roof
RS	0.75	/	/	Reflectance of the Shade Surface
TW	0.75	/	/	Transmissivity of Window
WT	0.2	/	m	Wall Thickness
WC	3	/	m	Width of Corridor



a). Visualization of parameters with random values in the interval

b). Visualization of parameters with fixed values

Fig. 3. The parameters visualization in parametric model.

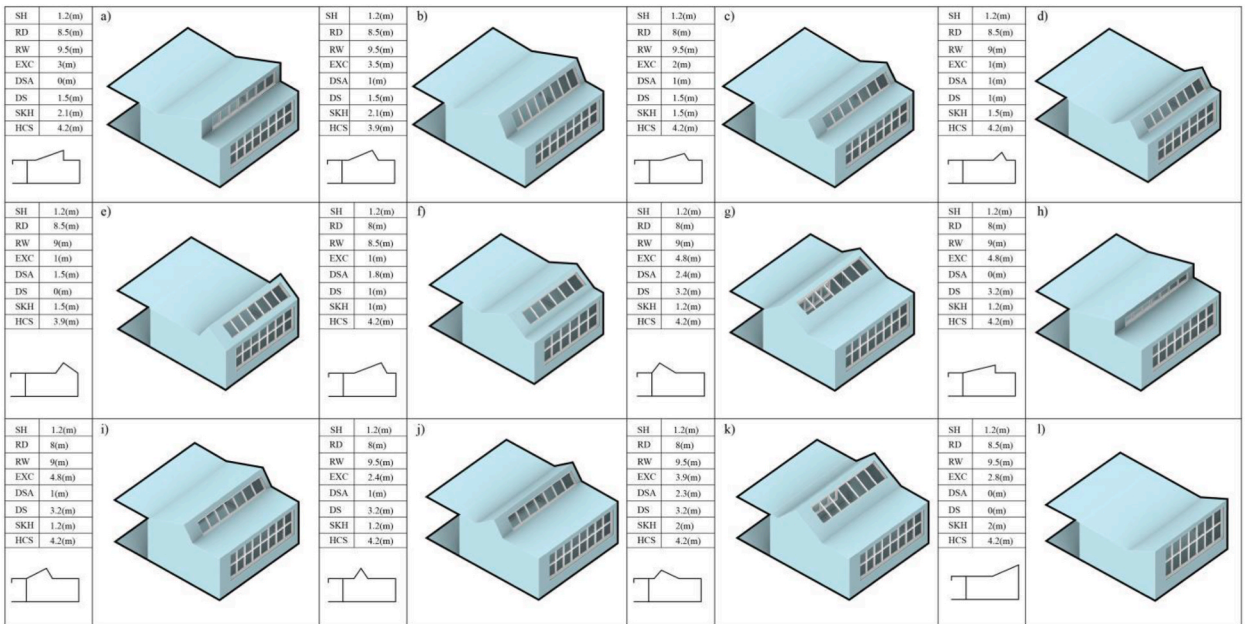


Fig. 4. Partial classroom configurations as parameters change.

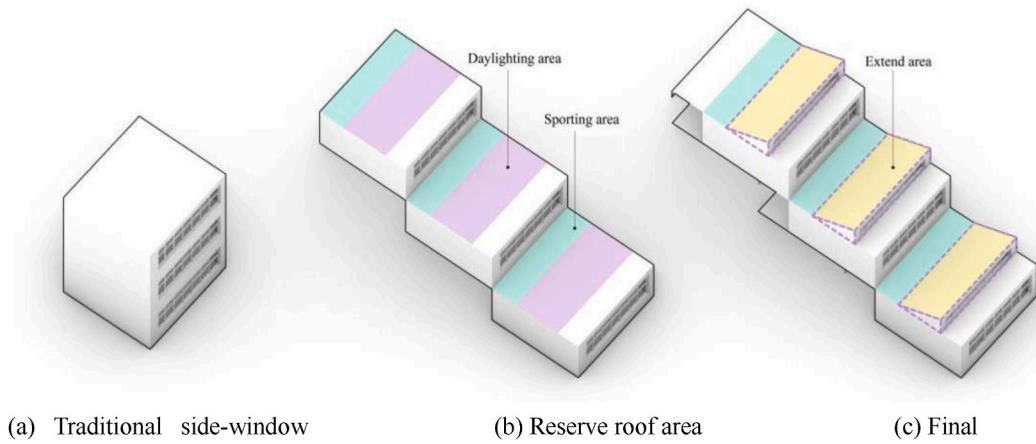


Fig. 5. Reserving the roof area of each layer by stepping back.

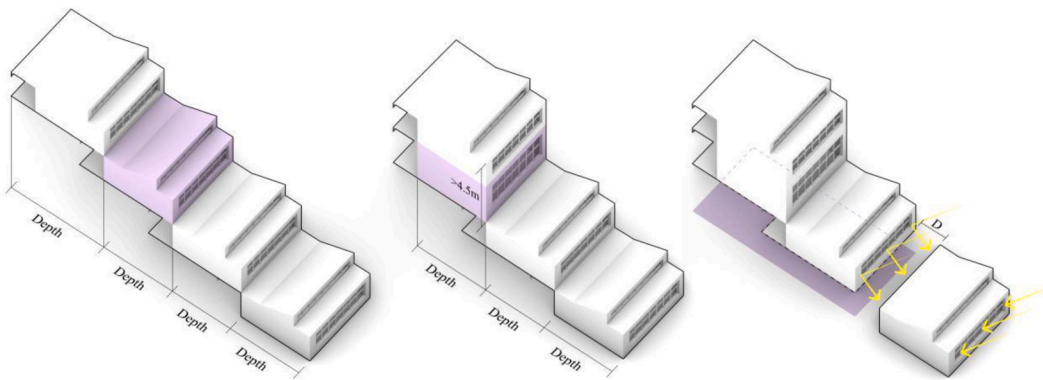


Fig. 6. Increase the height of third floor, first floor disconnected from the second floor.

skylight and enhance indoor daylighting performance, as depicted in Fig. 6. This approach also mitigates the negative impact of layer-upon-layer retreat on SU.

3.3.3. Adding atrium between the first floor and second floor

In addition to increasing the depth of the teaching building, the terraced layout also generates an elongated overhead space on one side of the ground floor. Although this approach enhances the amount of natural light received by the classrooms on each level, it does not favor the side lighting of the south-facing classrooms on the ground floor. To achieve bi-directional north-south lighting for the ground floor classrooms, as illustrated in Fig. 6, it is proposed to separate them from the second-floor classrooms. As a result, an atrium is introduced, which allows sunlight to penetrate into the south-facing classrooms on the ground floor. The role of the atrium in

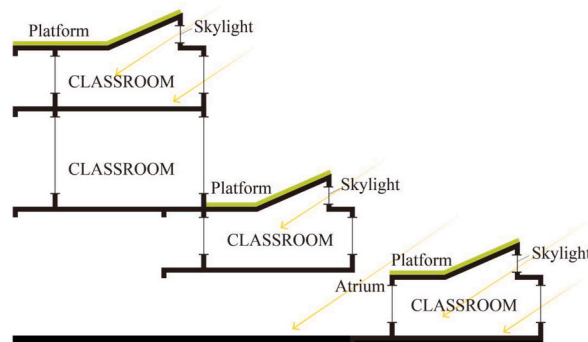


Fig. 7. The basic section.



relation to the classrooms has been previously identified in a study [58].

### 3.3.4. Generation of section and plane

The aforementioned set of three-generation rules are capable of generating basic terraced section units, as shown in Fig. 7. However, in order to account for the diversification of the design and the increase in data volume, certain modifications have been implemented. By reducing the number of classrooms, simultaneously, the alteration of skylight parameters and the relocation of the classroom can generate a multitude of novel profile forms, some of them are illustrated in depicted in Fig. 8.

During the creation of planar units, traditional classrooms have typically been designed with parallel and overlapping gable walls. In this experiment, the gable wall serves as an additional surface that can be utilized for installing high side windows to enhance natural light intake. The effective window area on the gable wall has been increased by controlling the length of the gable wall exposed to the outside of every two classrooms. Furthermore, each section unit has been staggered in the north-south direction. The displacement distance between two adjacent units is limited to the depth of one classroom at most. After the displacing, the gable wall of each classroom can expand the window area by incorporating high side windows. The GWL assessment in evaluating the effective surfaces on the gable walls is based on the summation of displacements between adjacent classrooms, with reference to the location of the first-floor classroom. The total displacement serves as a direct measure of the exposed area of gable walls to the outside, resulting in an increased number of effective surfaces on the gable walls.

### 3.4. Daylighting simulation

This paper conducted a daylighting simulation using the Ladybug tool 1.4, a Grasshopper plug-in, with the climate conditions in the Guangzhou area. The study select the sDA and ASE, which evaluate indoor daylighting conditions more comprehensively and realistically. The sDA is a percentage of the statistical space meeting the specified illuminance standard for more than 50% of the time in the year schedule under daylight alone, as defined by the Daylight Index Committee (IES-DMC) of the Illuminating Engineering Society of America in 2012. The ASE measures the possibility of visual discomfort in a space every year and represents the percentage of the area where the cumulative exposure time of the working plane reaches the specified number of hours under the established illuminance standard in the whole year. The UOD, which is the ratio of the minimum value of the daylight factor to the average value of it on the working plane, is selected as the primary reference index, in conjunction with the newly revised daylighting regulations in China [59].

The experiment was conducted at a height of 700 mm from the ground, and a plane test grid was established with a scale of 500 mm. The SDA calculation used a grid selected for the small and large sizes of the bottom classroom plane. The UOD was calculated only within the seating area. The test point was shifted inward by 1.5 m from the classroom edge. Preliminary experiments showed that traditional daylighting simulations took 1 min 53.8s to calculate the sDA, UOD, and ASE for a single room. The optimized shape in this study can contain up to 20 classrooms. If the conventional simulation method is used for a single simulation, it takes approximately 30 min. Therefore, an artificial neural network (ANN) prediction model was developed to improve the optimization efficiency in the later stages.

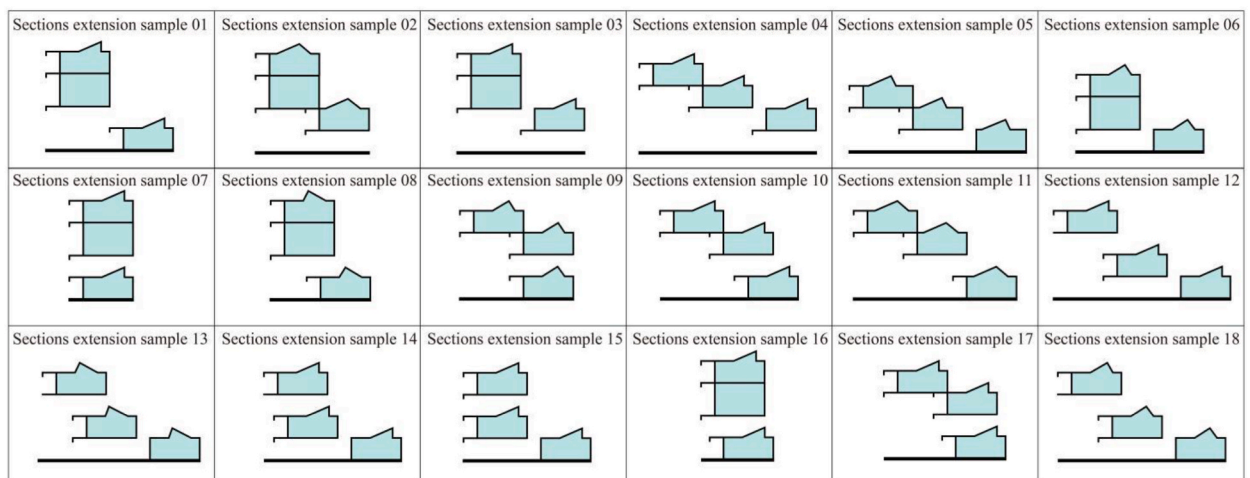


Fig. 8. Selected segments from the extended sections. To enhance the dataset’s robustness and diversity, classroom removal was employed to augment the number of training profiles. “Sections Extension Sample 01 through Sections Extension Sample 18 present 18 randomly generated outcomes resulting from variations in parameters.”

### 3.5. Sample simplification and ANN model

The combination of terraced structures creates complex shapes that can impact the daylighting of each classroom through occlusion and reflection from surrounding classrooms. Therefore, when constructing training samples for an artificial neural network (ANN) model, the distribution of neighboring classrooms is essential in addition to the relevant parameters of each individual classroom unit. However, encompassing all adjacent classrooms in the sample would considerably amplify its intricacy and the necessary computations. To simplify the training samples, this paper consider the influence of the surrounding environment of a single prediction unit first, as shown in Fig. 9a. Other classrooms within one width of the projection distance from the prediction unit are included in the range of influence factors of occlusion and reflection. Fig. 9b illustrates that there are 11 random location variables around each prediction unit, and the presence or absence of classrooms is represented as 1 or 0, respectively. In data processing, the center point of the bottom surface of the target unit was used as the origin and construct a coordinate system with the north-south direction as the y-axis and the east-west direction as the x-axis. Besides, taking the relative coordinates of the center points of the bottom surface of other units and arranging the position coordinates from west to east and bottom to top to obtain the sequential expansion of the positional relationship between the surrounding environment and the prediction unit. Since there are other influencing units on only one side of the end unit, only the influence of one side is considered in data processing, as shown in Fig. 9c, and the other side is expressed as 0. Secondly, for the group prediction problem facing multiple prediction units, we input the entire group as the input of the ANN by looping the environment around all units and the parameters of each unit itself. While it is important to highlight that, in order to enhance the prediction model's accuracy while simplifying the network structure, the network's output was limited to three values: sDa, ASE, and UOD. The two-dimensional matrix representing the distribution of light-harvesting planes was not included in the output, thus reducing complexity.

An Artificial Neural Network (ANN) is a prediction model composed of an input layer, a hidden layer, an output layer, and neuron nodes. The model functions by mapping the relationship between input and output data to achieve output results quickly. However, traditional daylighting simulations based on the Radiance engine are not ideal for real-time simulation due to the time-consuming of the ray-tracing algorithm. This problem can be effectively solved by using an ANN model.

In this experiment, as shown in Fig. 10 a fully connected feed-forward neural network with multiple hidden layers was chosen as the basis for the ANN model. The model was built based on the PyTorch framework, and Optuna was used for hyperparameter optimization. The output results include sDA, UOD and ASE. A simulation generated a total of 4000 samples.

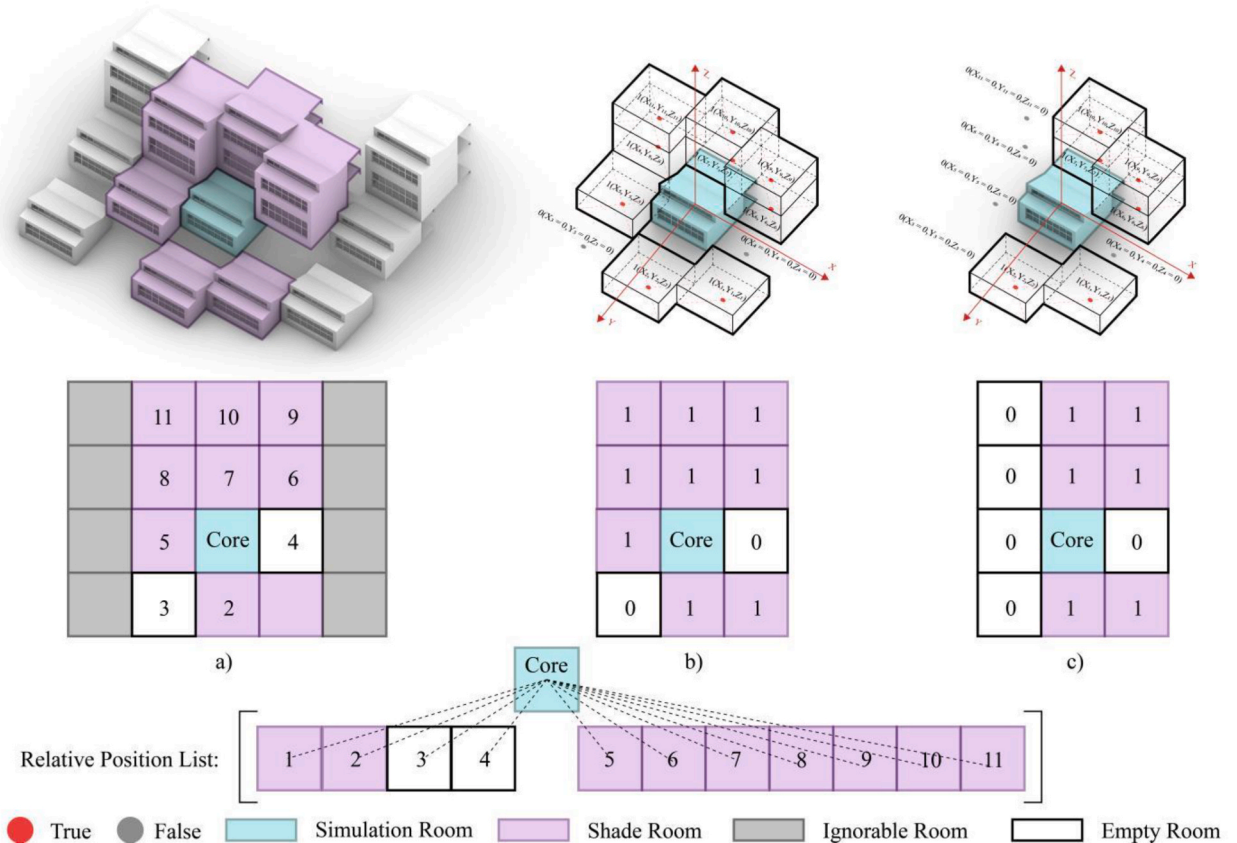


Fig. 9. Simplification of the sample.

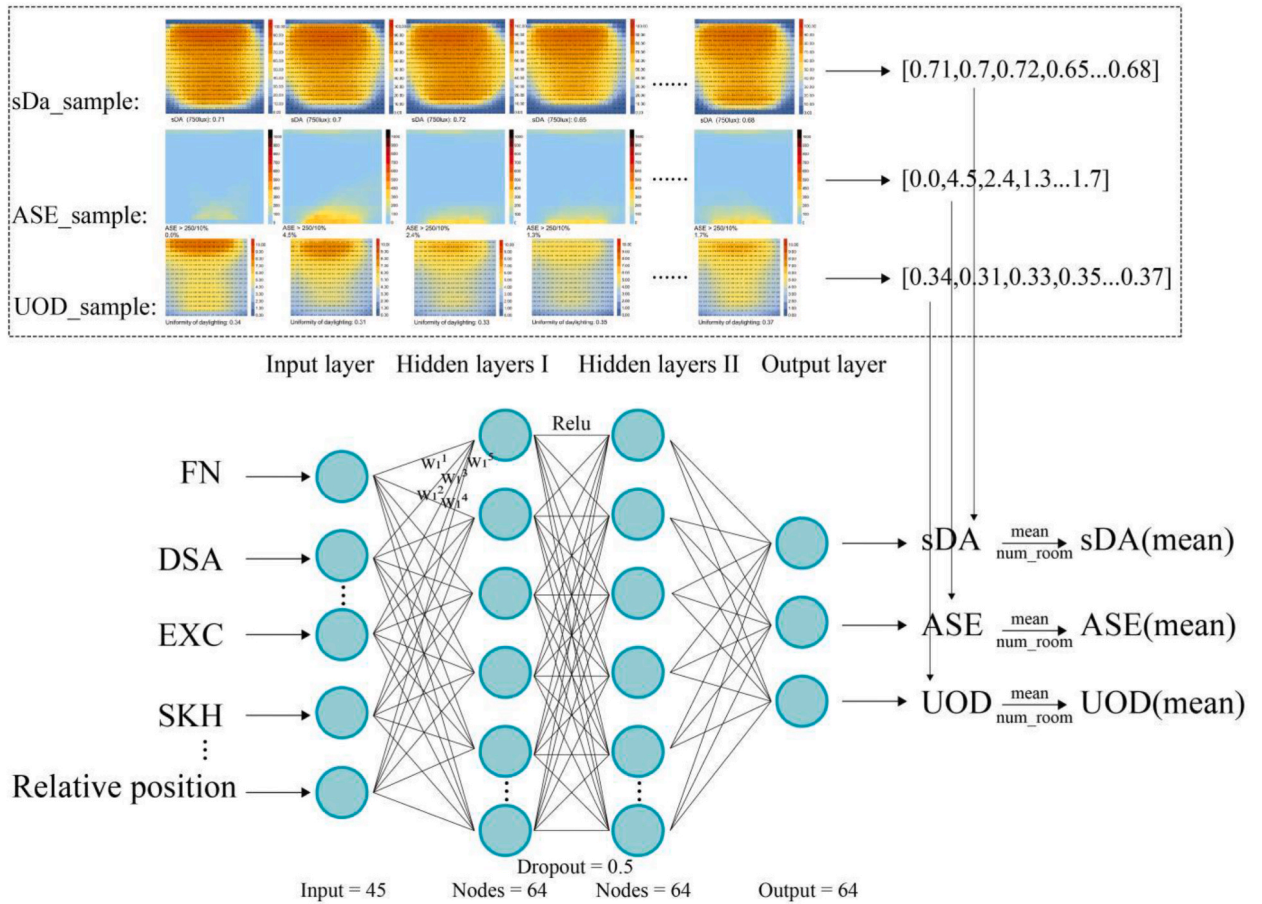


Fig. 10. ANN structure in training process.

### 3.6. Genetic algorithm multi-objective optimization

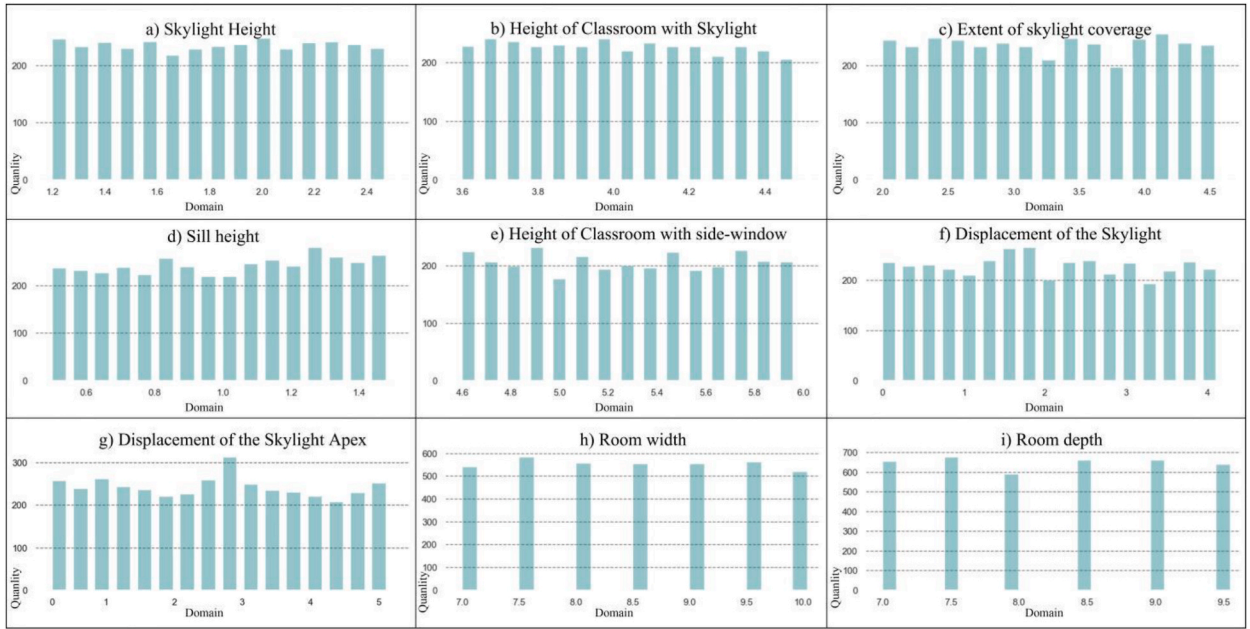
This study employed the Wallacei plug-in, which incorporates the NSGA-II (Non-Dominated Sorting Genetic Algorithm II), a commonly utilized multi-objective optimization algorithm, for optimization purposes. The trained artificial neural network model was integrated into the Grasshopper platform to accelerate the optimization process. The study focused on six optimization objectives, namely sDA, UOD, ASE, SU, GWL, and OPA. The former three objectives evaluated the overall daylighting performance. The SU aimed to ensure maximum Space utilization ratio, which guaranteed by minimizing the ratio between the maximum north-south depth and the number of classrooms contained in the form. GWL maximizes the total distance of mutual displacement of a one shape in optimization to obtain the most effective surface on the gables. Besides, In order to improve the optimization efficiency, the experiment reduced the search range and set a seed parameters that defined 1000 random combinations without any window parameters to limit the search space. In addition, to ensure that students have enough outdoor activity space, the OPA of each classroom is also taken as one of the optimization indicators.

The optimization process targeted a four-story terraced teaching building with five columns spanning from east to west on the north orientation. The six optimization objectives mentioned above are computed as the mean value across all classrooms within the building.

## 4. Result

### 4.1. Datasets description

The 4000-sample dataset comprises 1000 samples for each floor, ranging from the first floor to the fourth floor. As depicted in Fig. 11a–i, the primary dataset parameters exhibit a continuous random distribution within their respective intervals. However, RW and RD are discretized distributions, set as multiples of the simulated grid size, with a spacing of 0.5. Moreover, the samples were filtered according to generation rules in Grasshopper. Subsequently, Python was utilized to perform further filtration basing on a data structure consisting of 45 inputs and 3 outputs. This resulted in 3876 valid samples and 124 invalid samples out of the initial 4000



**Fig. 11.** Parameters distribution of all sample. The distribution of pertinent parameters within the designated interval of the training set. a–i respectively depict the distribution of each parameter’s value within the sample set.

samples. As a result, the training datasets consisted of 3100 samples, with 476 samples reserved for testing, and an additional 400 samples used for verification. Fig. 12a–c shows some training samples.

#### 4.2. ANN training result

##### 4.2.1. Hyperparameters optimization

The hyperparameters in machine learning, such as the number of hidden layers, neurons per layer, dropout probability, learning rate, and batch size, play a crucial role in determining the model’s accuracy. Finding the appropriate values for these hyperparameters is a critical task. Two common optimization methods for hyperparameters are Grid Search and Random Search. Grid Search exhaustively explores the search space by trying every combination of hyperparameter inputs, although it can be computationally expensive and less efficient. On the other hand, Random Search avoids unnecessary operations but is more likely to find locally optimal hyperparameter values. Both methods lack a structured approach to finding the optimal solution. Therefore, Bayesian optimization algorithm, implemented through Optuna, was utilized in this study to select hyperparameters, which has been demonstrated superiority over the aforementioned approaches [60].

The optimization process employed mean square error (MSE) (1) to evaluate objective and predicted values. Optimization iterations were set to 500 generations, and each iteration tested and evaluated 100 data sets. Results of the optimization process are presented in Fig. 13a–p, which indicates the loss values associated with various combinations of hyperparameters, the lighter colors indicate lower losses. The optimal hyperparameter combinations were obtained by combining the optimal values, with Table 2 showing the optimal value of each parameter.

$$MSE = \frac{1}{N} \sum_{i=1}^N (\hat{y}_i - y_i)^2 \tag{1}$$

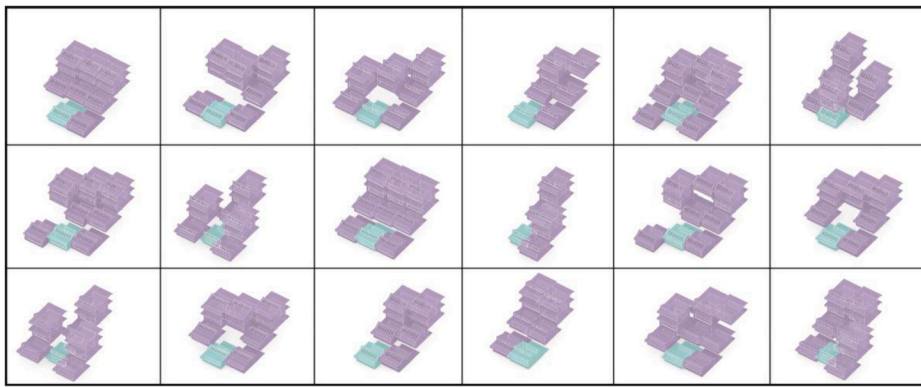
##### 4.2.2. ANN evaluation

The formally training was terminated after 600 generations. The training process is illustrated in Fig. 14.

The horizontal axis represents the number of iterations, while the vertical axis represents the loss. The blue line indicates the loss variation curve of the training set, and the red line represents the loss variation curve of the test set. After training, the training set loss was 0.00509, and the test set loss was 0.00556.

The trained model is evaluated using three indicators: MAE, RMSE, and R<sup>2</sup>. The result values are shown in Table 3, which reveals that both the UOD and sDa exhibit R2 values exceeding 0.8 in both the training and test datasets. On the other hand, the fit of ASE is inferior when compared to the aforementioned two variables. And Fig. 15a–f demonstrates the disparity between actual and predicted values through a scatter plot, affirming the model’s linear fit across both the training and test datasets. Therefore, although the model has some specific errors, it exhibits notable generalization capabilities and can potentially replace conventional daylighting simulation methods for predicting these three indicators.





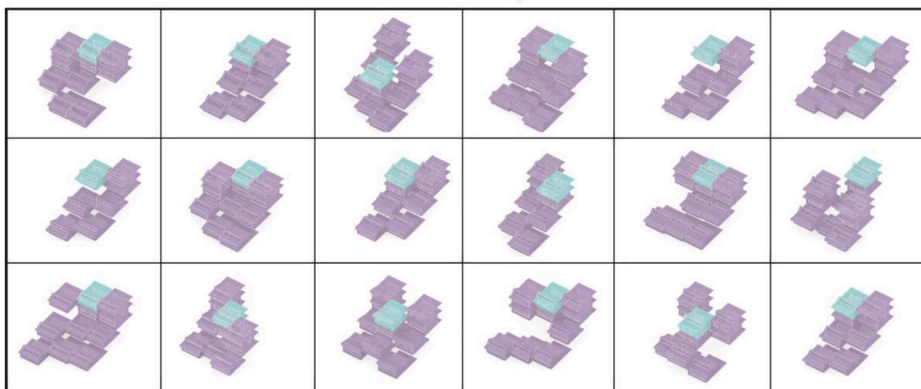
a) First floor sample



b) Second floor sample



c) Third floor sample



d) Fourth floor sample

(caption on next page)

Fig. 12. A part of training samples in each floor.

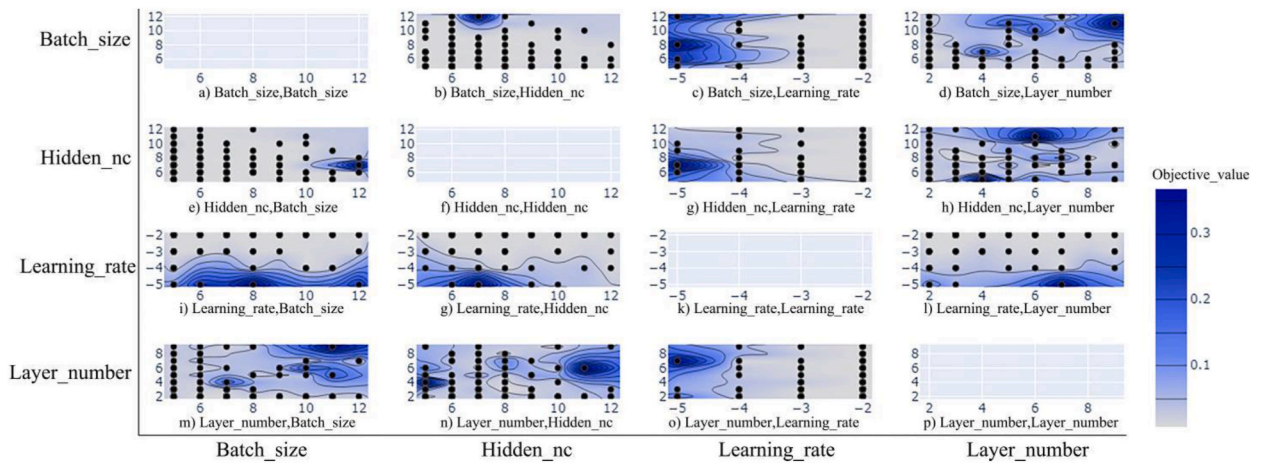


Fig. 13. Hyperparameters optimizing. a–p depict the contribution of various hyperparameters (Batch\_size, Hidden\_nc, Learning\_rate, Layer\_number) combinations to the target training value (Loss).

**Table 2**  
Values of hyperparameters.

Hyperparameter	Number	Explanation
Batch_size	2 <sup>6</sup>	The number of samples selected for one training
Hidden_nc	2 <sup>6</sup>	The number of neurons in each hidden layer
Learning_rate	1e <sup>-2</sup>	The learning rate
Layers_number	2	The number of the layer for the hidden layer

$$RMSE = \sqrt{\frac{1}{N} \sum_{i=1}^N (\hat{y}_i - y_i)^2} \tag{2}$$

$$MAE = \frac{1}{N} \sum_{i=1}^N |\hat{y}_i - y_i| \tag{3}$$

$$R^2 = 1 - \frac{\frac{1}{N} \sum_{i=1}^N (\hat{y}_i - y_i)^2}{\frac{1}{N} \sum_{i=1}^N (\hat{y}_i - \bar{y})^2} \tag{4}$$

Incorporate the ANN model into the Grasshopper platform. For each classroom unit in the prediction object, extract the parameter information through iterative looping. Subsequently, input this information into the ANN model and obtain the prediction results, which can grossly speed up the simulation. For instance, in the case of the four-story terraced teaching building with five east-west column spans, a single calculation requires only 5.6 s. This is 439 times faster than traditional daylighting simulations that take 41 min.

4.3. Assessment and analysis of multi-objective optimization results

4.3.1. The importance of feature analysis for parameters

This analysis calculated by the random forest algorithm, for the six targets is presented in Fig. 16a shows that the Displacement of the Skylight Apex (DSA) has the most significant impact on the sDA. This is because the DSA influences the daylighting area of the skylight, which affects the daylighting level in the space. The second factor involves Displacement of Skylight (DS), this is due to the ability of the skylight to illuminate the depths of the room through its displacement, and third factor is the set of 1000 randomly generated shape combinations, revealing the significant impact of complex shapes on lighting conditions as a result of shading and material reflection. This emphasizes the importance of considering these factors in lighting analysis. In panel Fig. 16b, the Room Depth (RD) has the most significant impact on the UOD, followed by DS. This is because a deeper space is less suitable for light to reach the interior, resulting in uneven illumination. SD can improve the illumination of deep spaces by positioning the skylight closer to the deep

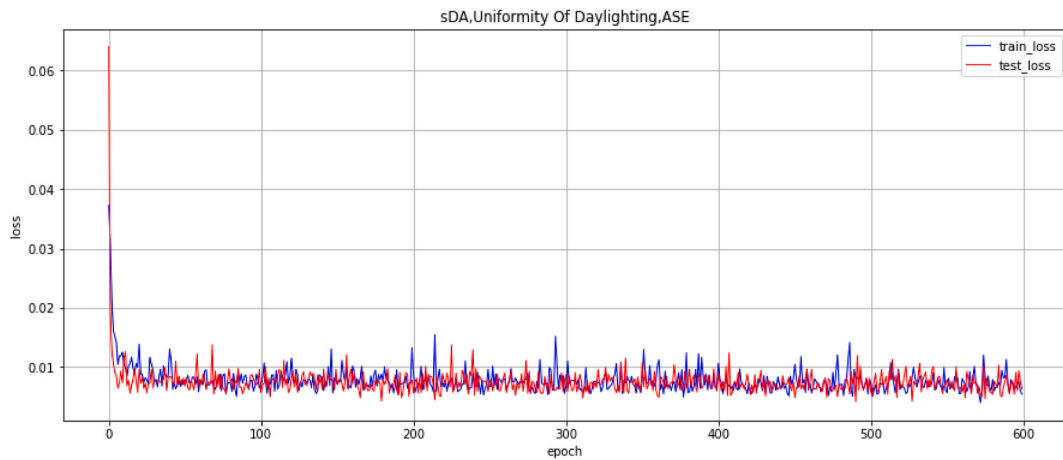


Fig. 14. Training process diagram.

space. Panel Fig. 16c reveals that the DSA has the most significant impact on ASE. In north-facing classrooms with limited direct sunlight, the majority of parameters exhibit negligible impacts on the ASE. However, as the DSA increases, the skylight gradually tilts, resulting in an enlarged illuminated area at the top and a higher solar altitude angle for direct light. This alteration notably enhances the illumination in certain indoor spaces, thereby leading to an augmented ASE. In Fig. 16d, DS has the most significant impact on the area of the outdoor activity platform, followed by Extent of Skylight Coverage (ESC), RD and RW. An increase in SD can divide the platform into two parts by the skylight, causing a first decrease and then an increase in the platform’s area. ESC reduces the sky

Table 3  
Performance of training and test model.

Index	Model	RMSE	MAE	R <sup>2</sup>
sDA	Train	0.040	0.033	0.858
	Test	0.046	0.036	0.806
UOD	Train	0.043	0.036	0.869
	Test	0.051	0.041	0.824
ASE	Train	2.827	2.089	0.809
	Test	3.684	2.319	0.755

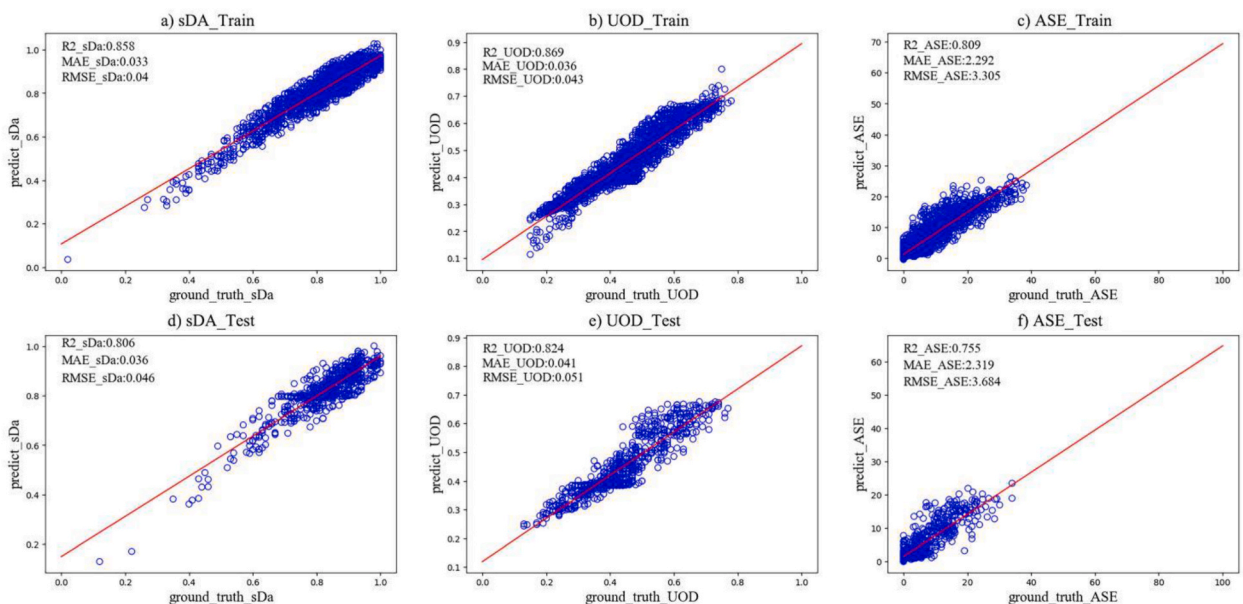


Fig. 15. ANN performance in training set (a–c) and testing set (d–f).

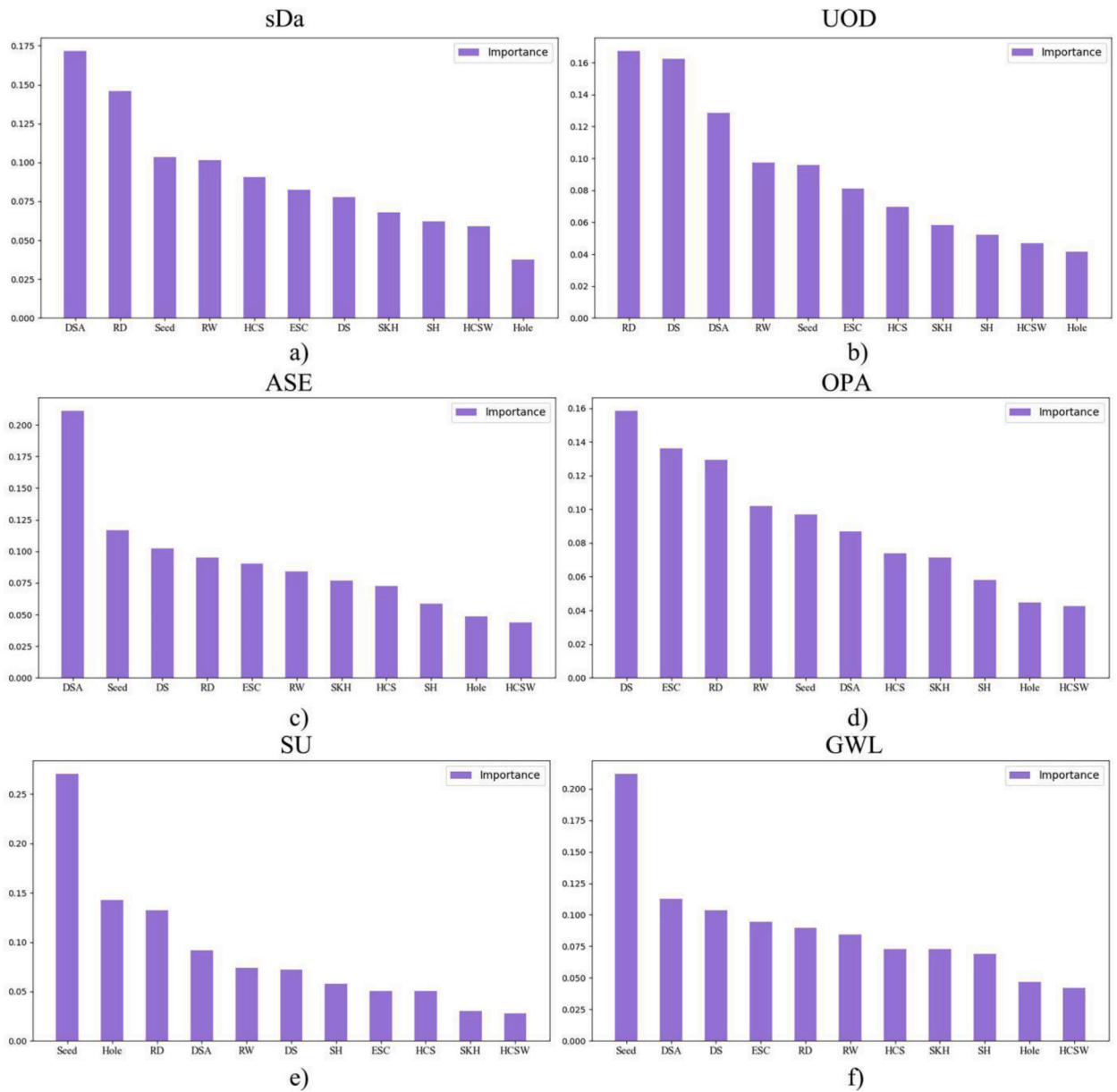


Fig. 16. Feature importance analysis. a-f sequentially delineate the hierarchical significance of design parameters influencing the six optimization objectives, namely sDA, UOD, ASE, OPA, SU, and GWL, throughout the optimization procedure.

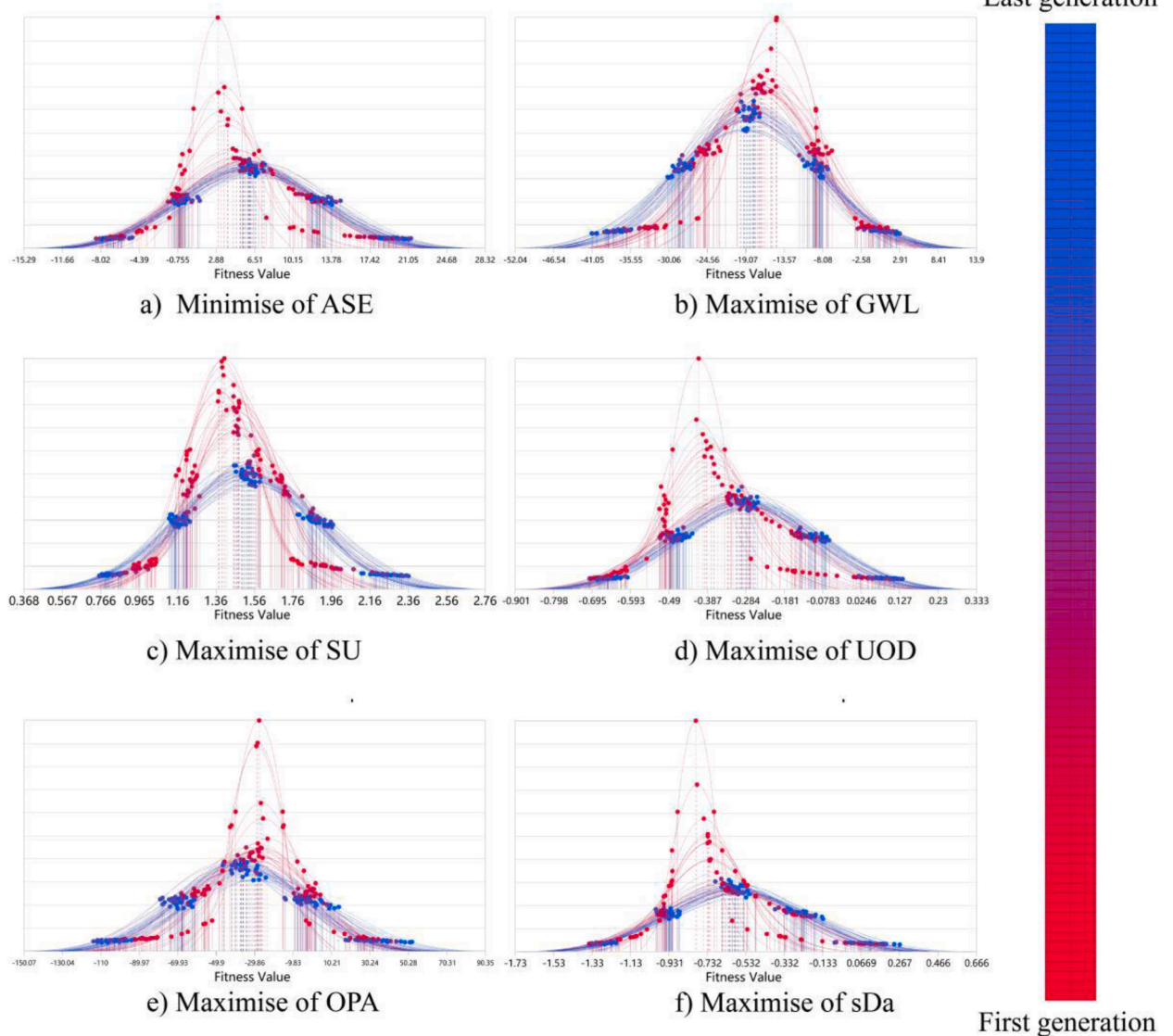
surface’s effective use area by changing the skylight’s coverage depth. RD and RW directly impact the top platform’s area by being related to the depth and width of the entire classroom. Finally, Fig. 16e and f show that the most impact on SU and the GWL are the seed parameters for these targets in the pre-set 1000 random combination shapes. These two items aim to select several optimal shape combinations from 1000 random shapes to achieve the best SU and GWL during the optimization process.

4.3.2. Results filtering

Fig. 17a–f depicts the distribution of standard deviation for the six optimization objectives throughout the optimization process. Each curve represents the distribution within a particular generation. The results reveal that as the optimization progresses, the standard deviation of the succeeding generation surpasses that of the preceding generation. This suggests a greater dispersion in the distribution of diverse solutions within the final optimized outcomes. Consequently, this study conducts additional screening based on these results. This process primarily focuses on three daylighting performance indicators: sDA, UOD, and ASE. Since there do not exist sDA specification in China, this paper defines sDA per the highest standard for daylighting with vertical or inclined walls described in “European Standard EN 17037” [61]: “95% of the area of a room is 50% of the time in a day. The illuminance exceeds 500 lx, and 50%



Last generation



**Fig. 17.** Stand deviation in optimizing process for six objectives. A–F respectively delineate the variations in standard deviation for ASE, GWL, SU, UOD, OPA, and sDA throughout the optimization procedure, aligned with their respective optimization objectives.

of the area illuminance exceeds 750 lx for 50% of the time.” However, the ANN model in this paper is trained under the threshold of 750 lux, it cannot evaluate under 500 lux, thus only uses 750 lux as a filter condition and improve the standard of it. The daylighting measure under the threshold of 750 lux is defined as “75% of the area of the room has an illuminance exceeding 750 lux in 50% of the time in a day.” UOD is defined per China’s “General Code for a Building Environment” [59], which requires that the UOD in ordinary classrooms should not be less than 0.5. ASE is primarily based on the requirements of the LEED (Leadership in Energy and Environmental Design) Association, with a primary reference of taking at most 10% of the area in the working plane to exceed 1000 lux in

**Table 4**  
Multi-objective screening results.

NO.	GWL	OPA	SU	UOD (mean)	ASE (mean)	sDA (mean)
1	17.82	33.6	1.5	0.60	6.72	0.92
2	36.15	40	2.03	0.50	7.60	0.76
3	14.1	27	1.16	0.63	6.25	0.92
4	11.32	33.6	1.3	0.60	5.46	0.89
Traditional	0	0	0.5	0.32	23.5	0.79

250 h per year [62]. Finally, the following filter mainly use three criteria of  $sDA_{750lux}$  greater than 0.75, UOD greater than 0.5, and  $ASE_{1000lux, 250h}$  less than 10%, resulting in four optimal solutions, as shown in Fig. 19. The indicator of each solution is presented in Tables 4 and 5 and their position on the Pareto chart is shown by Fig. 18, which is distributed on the Pareto hypersurface.

The screening results shown in Fig. 19 illustrate that the combination of north-oriented terrace classrooms significantly improves the OPA,  $sDa$ , UOD, and ASE compared to the traditional south-oriented side daylighting classrooms in primary and secondary schools, prior to optimization. Among these parameters, the most notable improvement is observed in the ASE. Direct sunlight in the south creates intense glare near the window, whereas the predominantly diffused sunlight received by the north-oriented terrace classrooms alleviates visual discomfort caused by direct sunlight. Additionally, UOD has shown significant improvement compared to the traditional classroom. During the experiment, it was evident that achieving a UOD exceeding 0.35 in side daylighting classrooms was challenging due to the shading of the corridor and the limited daylighting area on the side of the corridor, resulting in inadequate illuminance on this side of the classroom and uneven illuminance distribution throughout the space. The optimized design positions the skylights closer to the corridor side, allowing sunlight to penetrate into the classroom. This effectively addresses low illumination issues near the corridor side, resulting in uniform illuminance distribution throughout the classroom and an increased  $sDA$ . However, the terraced combination form occupies a larger space than the traditional form due to the presence of setbacks and a platform, which is a drawback. The terraced form occupies at least twice as much space as the traditional form. Despite occupying a larger space, the terraced form enhances the daylighting performance of the classrooms and provides a certain amount of outdoor activity space for each classroom. It also serves as a new reference model for the design of primary and secondary schools in the future.

## 5. Discussion

### 5.1. Optimization and simulation results compared for speed and accuracy

The simulations and experiments in this study were conducted using a computer equipped with an Intel(R) Core(TM) i7-9700F CPU operating at a main frequency of 3.00 GHz and an NVIDIA GeForce RTX 2060 graphics card. With the specified simulation parameters, the individual calculation times for  $sDa$ , UOD, and ASE in a single classroom unit were 1 min 05 s, 48 s, and 0.8 s, respectively, resulting in a total of 1 min 53.8 s. For group simulations, a four-story terraced school building with five column spans in the east-west direction was chosen, accommodating 18 to 20 classrooms. Each simulation calculation for this scenario typically required approximately 30 min. During the optimization process, a total of 5000 sets of simulations were compared for different parameter settings of the school building form. Using traditional simulation methods, this would have taken 2500 h. However, by deploying our trained model on the grasshopper platform, the time needed to iterate through all classroom parameters and calculate the output was reduced to only 5 s. After 5000 optimizations, the total time amounted to merely 7 h, resulting in a 357-fold acceleration.

The artificial neural network (ANN) model used in this study only provides three indicators ( $sDa$ , UOD, and ASE) to evaluate the overall indoor lighting condition, and it does not capture the lighting distribution at various test points within the room. Therefore, three classrooms were randomly selected from the four optimal solutions obtained for simulation using the traditional method. This approach served two purposes: firstly, to verify the accuracy of the results, and secondly, to observe the lighting distribution within the rooms. As shown in Fig. 20 (solution I–solution IV), the optimized results showed significantly smaller errors than ASE in terms of  $sDa$  and UOD, consistent with the fitting results of the ANN model presented in Table 3. Furthermore, the validation results from Fig. 20 (I\_3 and II\_3), which include three-story classrooms, indicated relatively larger errors for these classrooms. This discrepancy may be attributed to the limited representation of classrooms with high side windows in the sample set, leading to underfitting during the neural network fitting process. Therefore, the prediction error in this study primarily stems from the overestimation of UOD values for classrooms located on the third floor with side windows. Additionally, some classrooms show ASE errors.

Regarding the indoor distribution of Daylight Autonomy (Da), all classrooms with both skylights and side windows exhibited satisfactory performance. However, there was an exception for the darker region below the sill. Conversely, despite an increase in floor height, classrooms with skylights showed significantly better uniformity in the distribution of daylight factor (DF) compared to those with side windows. Additionally, the annual distribution of direct sunlight hours revealed that although there may not be significant direct sunlight exposure near the northern side windows, there is still some level of direct sunlight present in the lower section of the

**Table 5**  
Parameters related to the optimal solution.

NO.	Solution I	Solution II	Solution III	Solution IV
WH	1	0.8	1.1	1
Height I	4	4.1	4.1	4.1
SH	1.7	1.3	1.3	1.4
Height II	2.5	2.5	2.5	2.6
SL	3.3	3.3	4	3.2
Number	16	18	18	18
Tilt	2.3	2.3	1.5	1.4
SD	4.2	4	4.1	4.2
Width	8	10	9	9
Depth	7.5	10	7	7
Seed	6	458	75	13

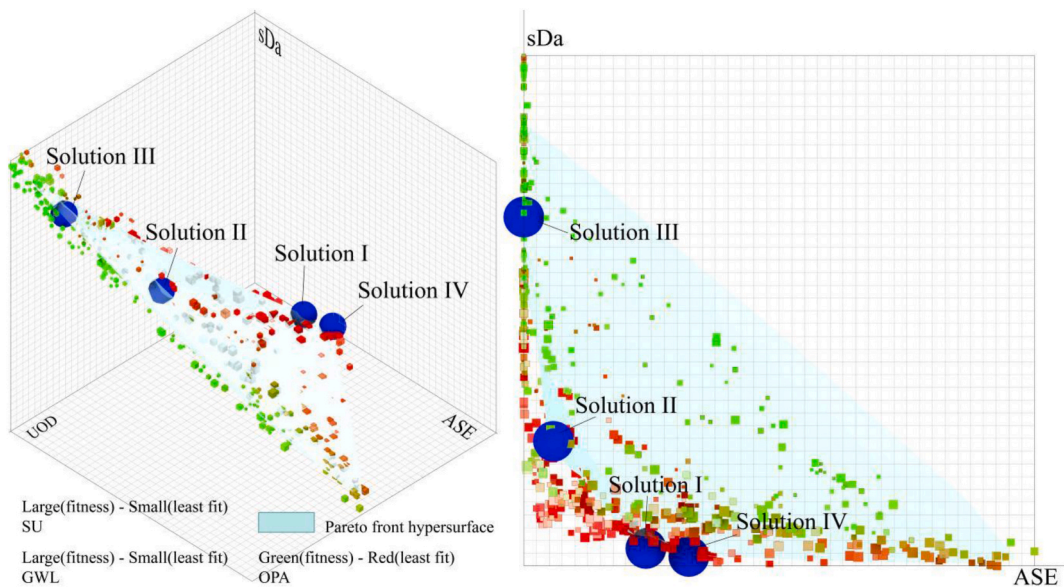


Fig. 18. Pareto-optimal solutions.

skylight.

### 5.2. Suggestions for classroom design based on daylighting in the future

Recommendations can be made to enhance classroom daylighting design in the post-epidemic era, based on the research presented in this paper. Optimal classroom unit designs that utilize skylight lighting or increased floor height with side windows can significantly enhance indoor sDa. Furthermore, to improve UOD within skylit classrooms, careful consideration of the integration of skylight parameters is necessary, including values such as SKH, DSA, EX, ESC, and DS. Among these parameters, it is recommended to position the skylight near the corridor. However, regarding the enhancement of UOD in classrooms equipped with high side windows, this study refrains from further exploring the topic due to experimental inaccuracies. Future studies may explore additional variables, such as the placement and size of side windows, as well as the ceiling arrangement. Additionally, in the case of north-facing classrooms, when tilted skylights are utilized, excessively steep angles can lead to direct light issues on the lower part. To mitigate this, the installation of lighting shelves beneath the skylight can be considered to prevent direct light penetration. Typically, classrooms with skylights exhibit superior daylighting performance compared to classrooms with side windows. Therefore, when conditions permit, skylight classrooms are recommended as the preferred option.

When considering classroom combinations, the utilization of terraced section proves advantageous in providing ample daylighting to each classroom while maintaining sufficient outdoor space, which will also aid in enhancing indoor air circulation to a certain degree. Moreover, due to the considerable spatial requirements of terraced classrooms, they pose significant challenges in terms of land usage and campus planning. Constructing buildings with this type necessitates more land and space, presenting an insurmountable obstacle for cities with limited land resources. Consequently, meticulous and scientifically informed considerations are imperative when opting for a terraced classroom design, encompassing campus planning, building design, and land utilization. And it is crucial to underscore that this model unquestionably offers a superior learning environment for students. Given that students spend a significant portion of their day in the classroom, the land limitations associated with this model can be addressed by effectively managing other areas within the site, such as incorporating additional multi-purpose spaces.

Furthermore, although the stepped arrangement increases the area of elevated windows on the gable wall, a comparison of solution3 and solution2 in the optimization results reveals that, despite solution2 having a larger GWL than solution3, the overall daylighting effectiveness of solution3 exceeds that of solution2. It is evident that the impact of GWL on daylighting performance is not the predominant factor. To confirm this, we conducted a reassessment of the significance of various factors influencing daylighting. The results, depicted in Fig. 21a–c, indicate that GWL ranks third in terms of its influence on sDa, with DSA and RW occupying the top two positions. Similarly, GWL ranks third in its influence on UOD, with RD and DS securing the top two ranks. Regarding the influence on ASE, GWL takes the second position, closely following DSA. Hence, the arrangement of planes can be flexibly customized to match the specific overall shape, traffic, and other requirements.

### 5.3. Limitation on the experiment

However, there are still limitations and areas for improvement in this experiment. First, all classrooms in the composite form are modular and use the same section type, which simplifies the model but imposes certain limitations. Therefore, future exploration can



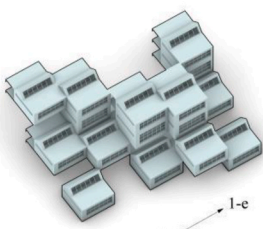
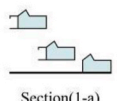
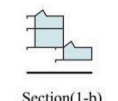
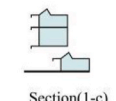
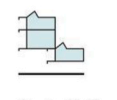
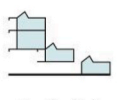
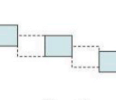
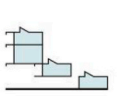
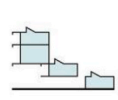
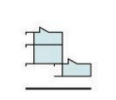
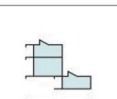
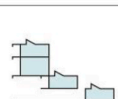
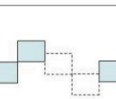
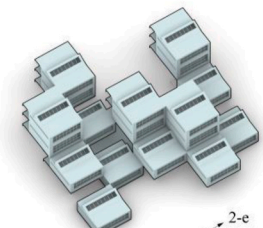
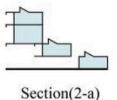
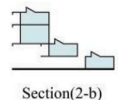
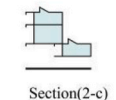
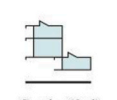
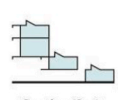
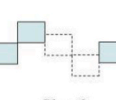
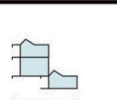


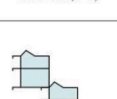
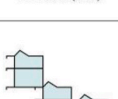
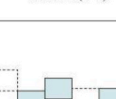
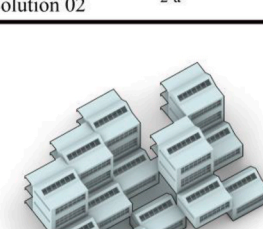
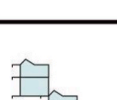
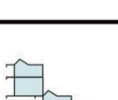

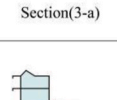
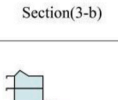
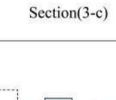
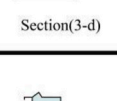
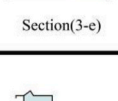
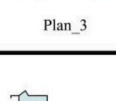
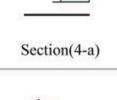
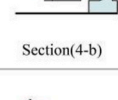
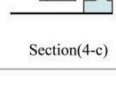
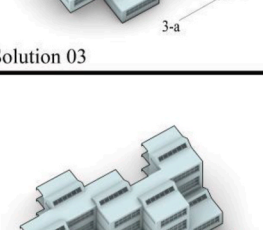
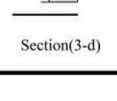
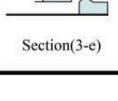
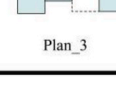
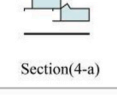
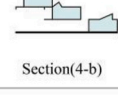
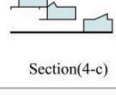
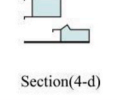
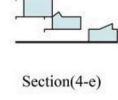
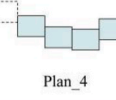
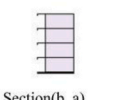
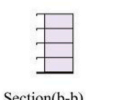
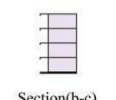
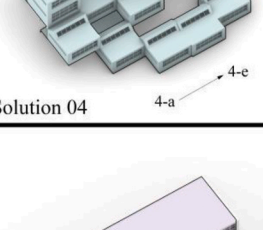
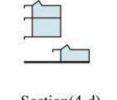
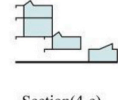
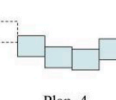
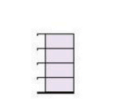


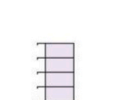
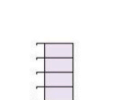
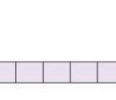
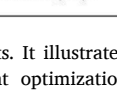
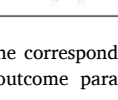
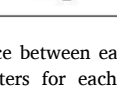
 <p>Solution 01</p> <p>1-a → 1-e</p>	 <p>Section(1-a)</p>	 <p>Section(1-b)</p>	 <p>Section(1-c)</p>	<p>1_First Floor</p>	sDA	0.92	○	0.92	○	0.90	
					UOD	0.63	○	0.57	○	0.63	
					ASE	5.79	○	3.49	○	5.40	
	 <p>Section(1-d)</p>	 <p>Section(1-e)</p>	 <p>Plan_1</p>	<p>1_Second Floor</p>	sDA	0.92	○	0.91	○	0.94	0.90
					UOD	0.66	0.64	○	0.61	0.63	
					ASE	5.79	6.12	○	8.97	5.56	
	 <p>Section(1-d)</p>	 <p>Section(1-e)</p>	 <p>Plan_1</p>	<p>1_Third Floor</p>	sDA	○	0.91	0.92	○	0.94	0.91
					UOD	○	0.47	0.49	0.48	0.50	
					ASE	○	5.99	6.09	9.72	5.64	
	 <p>Section(1-d)</p>	 <p>Section(1-e)</p>	 <p>Plan_1</p>	<p>1_Fourth Floor</p>	sDA	0.92	0.90	0.92	0.95	0.91	
					UOD	0.66	0.65	0.67	0.68	0.66	
					ASE	7.34	6.62	5.99	11.79	7.18	
 <p>Solution 02</p> <p>2-a → 2-e</p>	 <p>Section(2-a)</p>	 <p>Section(2-b)</p>	 <p>Section(2-c)</p>	<p>2_First Floor</p>	sDA	0.84	0.45	○	○	0.66	
					UOD	0.48	0.39	○	○	0.51	
					ASE	9.41	1.72	○	○	4.61	
	 <p>Section(2-d)</p>	 <p>Section(2-e)</p>	 <p>Plan_2</p>	<p>2_Second Floor</p>	sDA	0.84	0.44	0.96	0.98	0.67	
					UOD	0.52	0.39	0.63	0.58	0.41	
					ASE	11.91	2.06	12.45	12.71	4.61	
	 <p>Section(2-d)</p>	 <p>Section(2-e)</p>	 <p>Plan_2</p>	<p>2_Third Floor</p>	sDA	0.92	0.45	0.92	0.95	0.62	
					UOD	0.41	0.52	0.41	0.42	0.48	
					ASE	7.68	2.29	5.86	7.41	5.76	
	 <p>Section(2-d)</p>	 <p>Section(2-e)</p>	 <p>Plan_2</p>	<p>2_Fourth Floor</p>	sDA	0.92	0.47	0.93	0.95	0.61	
					UOD	0.58	0.40	0.61	0.61	0.61	
					ASE	15.26	2.78	10.34	13.93	5.28	
 <p>Solution 03</p> <p>3-a → 3-e</p>	 <p>Section(3-a)</p>	 <p>Section(3-b)</p>	 <p>Section(3-c)</p>	<p>3_First Floor</p>	sDA	○	0.92	0.93	○	0.94	
					UOD	○	0.65	0.67	○	0.67	
					ASE	○	6.62	7.32	○	9.06	
	 <p>Section(3-d)</p>	 <p>Section(3-e)</p>	 <p>Plan_3</p>	<p>3_Second Floor</p>	sDA	0.95	0.92	0.93	0.92	0.92	
					UOD	0.68	0.66	0.68	0.65	0.65	
					ASE	10.36	5.75	6.61	6.79	6.83	
	 <p>Section(3-d)</p>	 <p>Section(3-e)</p>	 <p>Plan_3</p>	<p>3_Third Floor</p>	sDA	0.94	0.88	0.90	0.87	0.92	
					UOD	0.53	0.53	0.59	0.56	0.56	
					ASE	8.89	4.28	5.59	4.26	6.24	
	 <p>Section(3-d)</p>	 <p>Section(3-e)</p>	 <p>Plan_3</p>	<p>3_Fourth Floor</p>	sDA	0.94	0.87	0.92	0.88	0.93	
					UOD	0.69	0.68	0.68	0.66	0.65	
					ASE	9.66	7.29	5.96	4.41	7.29	
 <p>Solution 04</p> <p>4-a → 4-e</p>	 <p>Section(4-a)</p>	 <p>Section(4-b)</p>	 <p>Section(4-c)</p>	<p>4_First Floor</p>	sDA	○	0.90	0.90	0.91	0.91	
					UOD	○	0.64	0.63	0.62	0.60	
					ASE	○	5.16	6.60	5.54	6.87	
	 <p>Section(4-d)</p>	 <p>Section(4-e)</p>	 <p>Plan_4</p>	<p>4_Second Floor</p>	sDA	0.87	0.91	0.91	○	0.87	
					UOD	0.63	0.64	0.63	○	0.66	
					ASE	1.79	4.94	4.89	○	1.66	
	 <p>Section(4-d)</p>	 <p>Section(4-e)</p>	 <p>Plan_4</p>	<p>4_Third Floor</p>	sDA	0.89	0.90	0.88	0.88	0.89	
					UOD	0.48	0.56	0.59	0.58	0.50	
					ASE	2.78	4.11	2.95	3.53	3.01	
	 <p>Section(4-d)</p>	 <p>Section(4-e)</p>	 <p>Plan_4</p>	<p>4_Fourth Floor</p>	sDA	0.88	0.91	0.90	0.89	0.90	
					UOD	0.66	0.65	0.62	0.66	0.66	
					ASE	7.02	7.72	6.41	7.55	6.90	
 <p>Before</p> <p>b-a → b-e</p>	 <p>Section(b_a)</p>	 <p>Section(b_b)</p>	 <p>Section(b_c)</p>	<p>b_First Floor</p>	sDA	0.75	0.76	0.75	0.77	0.75	
					UOD	0.29	0.30	0.28	0.28	0.30	
					ASE	22.72	21.02	21.56	22.76	22.86	
	 <p>Section(b_d)</p>	 <p>Section(b_e)</p>	 <p>Plan_b</p>	<p>b_Second Floor</p>	sDA	0.80	0.82	0.83	0.82	0.82	
					UOD	0.31	0.32	0.31	0.32	0.33	
					ASE	23.36	24.41	23.96	22.47	23.24	
	 <p>Section(b_d)</p>	 <p>Section(b_e)</p>	 <p>Plan_b</p>	<p>b_Third Floor</p>	sDA	0.83	0.84	0.82	0.83	0.82	
					UOD	0.32	0.33	0.32	0.33	0.32	
					ASE	24.74	23.38	24.96	24.73	24.19	
	 <p>Section(b_d)</p>	 <p>Section(b_e)</p>	 <p>Plan_b</p>	<p>b_Fourth Floor</p>	sDA	0.83	0.83	0.82	0.83	0.82	
					UOD	0.33	0.34	0.32	0.32	0.33	
					ASE	24.86	24.41	23.81	24.37	23.12	

Fig. 19. Multi-objective filtering results. It illustrates the correspondence between each solution (01–04) and its respective section and plane. Furthermore, it presents the pertinent optimization outcome parameters for each classroom and juxtaposes these results with the pre-optimization benchmarks.



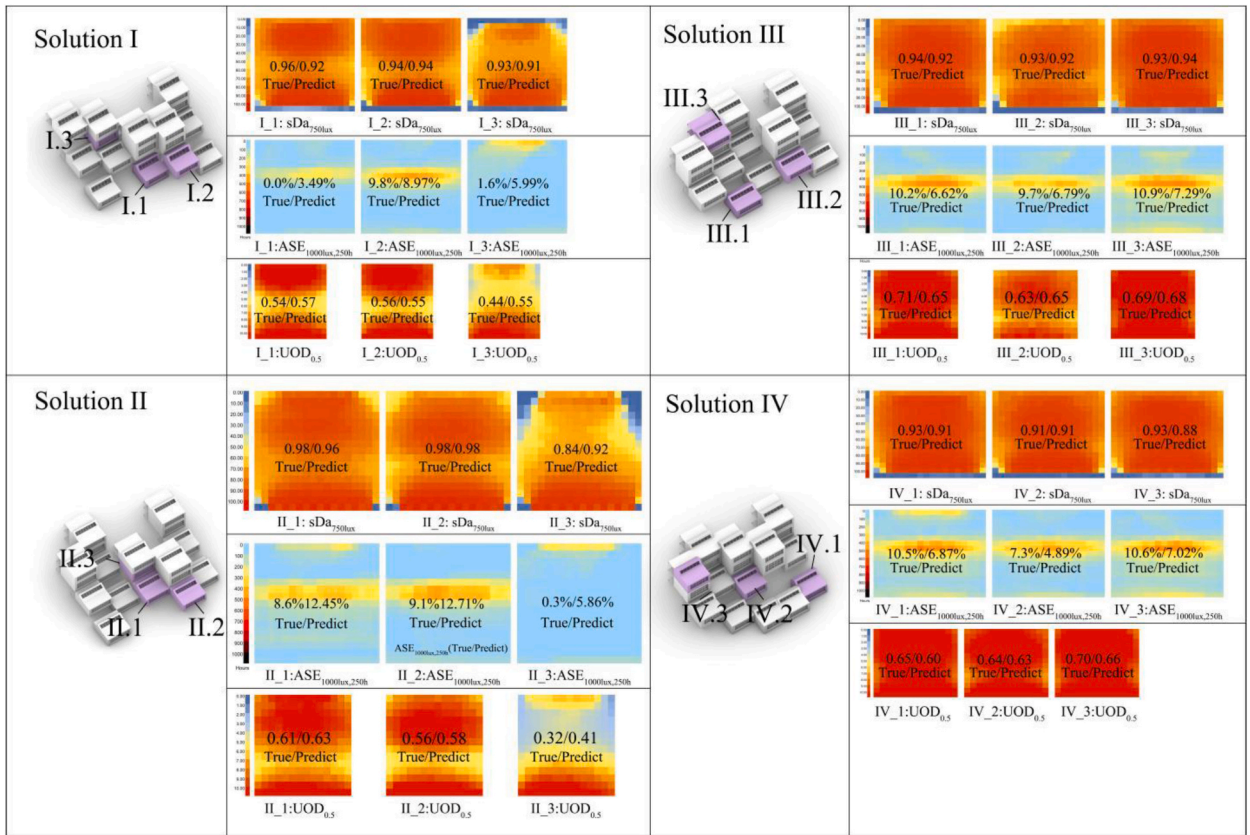


Fig. 20. The validation of optimization results. Three rooms were meticulously chosen at random for each proposed solution (I–IV) to rigorously assess the indicators of sDa, ASE, and UOD, thereby providing a comprehensive evaluation of the daylighting distribution.

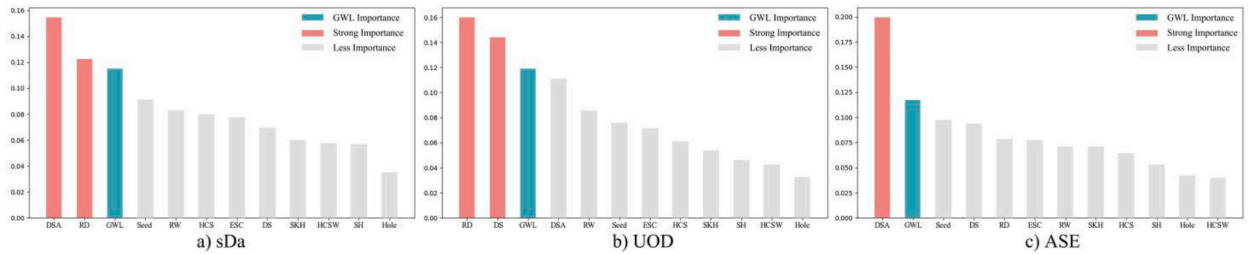


Fig. 21. The GWL impact on three indices. a–c respectively delineate the hierarchical impact of GWL on the three evaluative indicators: sDa, UOD, and ASE.

focus on incorporating various classroom sections into a combined shape. Secondly, the generation rules of the terraced combination stipulate that the depth of one classroom should be set back from the first floor, resulting in an excessively long depth direction for the entire form and leading to a low SU. Therefore, further discussion on the setback distance is needed. For instance, optimizing the overall shape could involve striking a balance between the setback distance of classrooms on each floor and the size and form of skylights.

To simplify the optimization model in the experiment, the overall daylighting performance of the space is evaluated using the sDa, UOD, and ASE trained by the ANN model. The average value of all classrooms provides an evaluation of the daylighting performance for the entire building. However, it is important to note that these metrics have limitations when assessing the daylighting distribution on specific surfaces. Therefore, while these mean metrics can offer a general assessment of the daylighting performance of a building, they may have limitations when more detailed information on the daylighting distribution is required. Furthermore, the low prediction accuracy of ASE becomes apparent when training the three indicators together in a single neural network. This discrepancy may arise from significant variations in the sample values across different indicators. Therefore, it is advisable to train indicators with significant differences separately in subsequent experiments.

Upon examining the final optimization results, it became evident that none of the four proposed solutions considered critical factors such as vertical structure, traffic flow, and evacuation on the same floor. Furthermore, the skylight's width was identical to that of the classroom, obstructing access to the outdoor platform from within the classroom. Therefore, it is suggested that subsequent studies consider the width of the skylight as a crucial parameter and simultaneously incorporate measures for structural integrity as well as vertical and horizontal traffic flow controls to address these issues. Additionally, to address the potential impact of heat radiation on indoor comfort, this experiment focused solely on a specific room layout on the north side, neglecting other layout types such as south-facing rooms. Future studies could explore various layouts, including those incorporating sunshade components, indoor thermal environment control, and other features such as different types of corridors and orientations.

## 6. Conclusion

In light of the post-epidemic scenario, this study reevaluates the existing classroom layout in primary and secondary schools with a focus on health considerations. The research delves deeper into the incorporation of multi-level classrooms that prioritize optimal daylighting performance during the initial design stage, taking into account the climatic conditions of the Guangzhou region and drawing insights from previous experiences in school design during epidemics. Additionally, it considers exemplary cases of daylighting design to ensure sufficient indoor natural light and outdoor activity spaces.

To overcome the time-consuming nature of traditional lighting simulations, this study proposes an artificial neural network (ANN) prediction model that can effectively handle complex shapes and multiple lighting indicators. The trained model predicts sDa, UOD, and ASE, showing a relatively weaker fit for ASE compared to the other two indicators. Additionally, the fit for three-story side window classrooms, which had a smaller sample size, was not as strong as that for skylight classrooms. Implementing the trained model in Grasshopper using Python significantly accelerated the runtime, achieving a speed improvement of 357 times compared to the traditional method. Building upon this premise, a multi-objective optimization was conducted, and the resulting optimal solutions were subsequently evaluated based on the aforementioned three primary daylighting indicators and relevant criteria. As a result, four optimal solutions were obtained. The outcomes demonstrate that integrating skylights into the terraced classroom design can greatly improve the overall daylighting performance within the space, surpassing that of conventional school buildings. Specifically, both sDa and ASE demonstrate excellent performance. Although UOD performs well in skylight classrooms, further improvements are necessary for high side window classrooms. However, the impact of high side window lighting on the gable wall (GWL) appears to be minimal.

In summary, this study successfully achieves a harmonious balance between captivating building form and daylighting performance. The proposed combination of terraced forms creates favorable indoor daylighting and outdoor spaces that provide students in the post-epidemic era with access to abundant natural light. These findings offer valuable insights for decision-making in the initial stages of the design process.

## Data availability statement

Data will be made available on request.

## CRediT authorship contribution statement

**Yubo Liu:** Supervision, Resources, Investigation, Funding acquisition, Conceptualization. **Kaifan Chen:** Writing – review & editing, Writing – original draft, Visualization, Validation, Software, Methodology, Investigation, Formal analysis, Data curation. **Eryu Ni:** Writing – review & editing, Writing – original draft, Supervision, Resources, Project administration. **Qiaoming Deng:** Resources, Methodology, Investigation, Funding acquisition, Conceptualization.

## Declaration of competing interest

The authors declare the following financial interests/personal relationships which may be considered as potential competing interests: Yubo Liu reports financial support was provided by National Natural Science Foundation of China. Qiaoming Deng reports financial support was provided by National Natural Science Foundation of China. Yubo Liu reports financial support was provided by State Key Lab of Subtropical Building Science.

## Acknowledgments

The work was supported by the National Natural Science Foundation of China, China under Grant No. 51978269 & No. 51978268.

## References

- [1] H.J. Moriske (Ed.), *Stellungnahme der Kommission Innenraumlufthygiene am Umweltbundesamt, Umweltbundesamt, Dessau-Roßlau, Germany, 2020.*
- [2] Y. Al Horr, M. Arif, M. Katafygiotou, A. Mazroei, A. Kaushik, E. Elsarag, *Impact of indoor environmental quality on occupant well-being and comfort: a Review of the Literature*, *Int. J. Sustain. Built. Environ.* 5 (2016) 1–11.
- [3] N.E. Klepeis, W.C. Nelson, W.R. Ott, J.P. Robinson, A.M. Tsang, P. Switzer, J.V. Behar, S.C. Hern, W.H. Engelmann, *The national human activity pattern survey (NHAPS): a resource for assessing exposure to environmental pollutants*, *J. Expo. Sci. Environ. Epidemiol.* 11 (2001) 231–252.
- [4] K.M. Zielinska-Dabkowska, K. Xavia, *Protect our right to light*, *Nature* 568 (7753) (2019) 451–453.

- [5] L. Heschong, Daylighting in Schools an Investigation into the Relationship between Daylighting and Human Performance Condensed Report, 1999 [cited 2023 Jan 29]; Available from: .
- [6] Boyce P, Hunter C, Howlett O. The Benefits of Daylight through Windows.
- [7] M.B. Ariès, M.P. Aarts, J. van Hoof, Daylight and health: a review of the evidence and consequences for the built environment, *Light. Res. Technol.* 47 (1) (2015) 6–27, <https://doi.org/10.1177/1477153513509258>.
- [8] J. Zhang, K. Lv, X. Zhang, M. Ma, J. Zhang, Study of human visual comfort based on sudden vertical illuminance changes, *Buildings* 12 (8) (2022).
- [9] IEEE Recommended Practices for Modulating Current in High-Brightness LEDs for Mitigating Health Risks to Viewers, IEEE, 2015, pp. 1–80.
- [10] T.A. LeGates, C.M. Altimus, H. Wang, H. Lee, S. Yang, H. Zhao, A. Kirkwood, E.T. Weber, S. Hattar, Aberrant light directly impairs mood and learning through melanopsin-expressing neurons, *Nature* 491 (7425) (2012) 594–598.
- [11] P.F. Yuan, Y. Song, Y. Lin, H.S. Beh, Y. Chao, T. Xiao, S. Huang, J. Zheng, Z. Wu, An architectural building cluster morphology generation method to perceive, derive, and form based on cyborg-physical wind tunnel (CPWT), *Build. Environ.* 203 (2021), 108045, <https://doi.org/10.1016/j.buildenv.2021.108045>.
- [12] Z. Li, H. Chen, B. Lin, Y. Zhu, Fast bidirectional building performance optimization at the early design stage, *Build. Simulat.* 11 (2018) 647–661, <https://doi.org/10.1007/s12273-018-0432-1>.
- [13] C. Huang, G. Zhang, J. Yao, X. Wang, J.K. Calautit, C. Zhao, et al., Accelerated environmental performance-driven urban design with generative adversarial network, *Build. Environ.* 224 (2022), 109575.
- [14] R. Crowley, The open-air school movement, *Br. J. Tubercul.* 3 (3) (1909) 188–190.
- [15] F. Clay, *Modern School Buildings, Elementary and Secondary: A Treatise on the Planning, Arrangement, and Fitting of Day and Boarding Schools, Having Special Regard to School Discipline, Organisation, and Educational Requirements; with Special Chapters on the Treatment of Class Rooms, Lighting, Warming, Ventilation, and Sanitation* [Internet], B.T. Batsford, 1902. Available from: <https://books.google.com.hk/books?id=pJbFAAAMAAJ>.
- [16] J. Liu, Changes in school design under the concept of health: the open-air school movement in the early 20th century and its design implications, *Huazhong Archit.* 40 (11) (2022) 64–68.
- [17] J. Liu, Changes in the design of “windowless classroom” of primary and secondary schools in the United States, *Huazhong Archit.* 40 (4) (2022) 127–131.
- [18] K.T. Tikkanen, Significance of Windows in Classrooms, University of California, Berkeley (CA), 1970 [dissertation].
- [19] B.M. Romney, The Effects of Windowless Classrooms on the Cognitive and Affective Behavior of Elementary School Students, University of New Mexico, 1972.
- [20] D. Guyon, Daylight dividends case study: Smith Middle School, Chapel Hill, NC, *J. Green Build.* 1 (1) (2006) 33–38.
- [21] R.P. Leslie, *Guide for Daylighting School*, Lighting Research Center, NY, 2004.
- [22] Department for Education and Employment, *Building Bulletin 90: Lighting Design for Schools*, 1999.
- [23] R. Koti, B. Architect, M. Munshi, Daylighting analysis of a classroom space using BIM geometry and next generation metrics, in: 38th ASES National Solar Conference, 2009, pp. 538–559.
- [24] M. Nicklas, U. Atre, Comparison of daylighting strategies for schools, in: PROCEEDINGS OF THE SOLAR CONFERENCE, 1, American Solar Energy Society; American Institute of Architects, 2007, p. 428.
- [25] M.H. Nicklas, G.B. Bailey, Analysis of the Performance of Students in Daylit Schools, 1996.
- [26] H. Eckerlin, M. Manning, U. Atre, et al., A new daylighting strategy for a middle school in North Carolina, in: Proceedings of the Solar Conference, 2, American Solar Energy Society; American Institute of Architects, 2007, p. 734.
- [27] D.H.R. Spennemann, Designing for COVID-2x: reflecting on future-proofing human habitation for the inevitable next pandemic, *Buildings* 12 (7) (2022).
- [28] L. Hermann, The Hygiene of the Eye in Schools, 1886.
- [29] L. Moretti, *Ricerca matematica in architettura e urbanistica*, *Moebius IV* 1 (1971) 30–53.
- [30] Y.E. Kalay, *Modeling Objects and Environments*, 1989.
- [31] Nicklas M, Design I. National Best Practices Manual for Building High Performance Schools.
- [32] X. Yu, Y. Su, X. Chen, Application of RELUX simulation to investigate energy saving potential from daylighting in a new educational building in UK, *Energy Build.* 74 (2014) 191–202.
- [33] ASHRAE, Standard 100-2018 – Energy Efficiency in Existing Buildings, 2017 (ANSI Approved/IES Co-sponsored).
- [34] K. Lakhdari, L. Sriti, B. Painter, Parametric optimization of daylight, thermal and energy performance of middle school classrooms, case of hot and dry regions, *Build. Environ.* 204 (2021 Oct), 108173.
- [35] P. Bakmohammadi, E. Noorzai, Optimization of the design of the primary school classrooms in terms of energy and daylight performance considering occupants’ thermal and visual comfort, *Energy Rep.* 6 (2020 Nov) 1590–1607.
- [36] A. Zhang, R. Bokel, A. van den Dobbelen, Y. Sun, Q. Huang, Q. Zhang, Optimization of thermal and daylight performance of school buildings based on a multi-objective genetic algorithm in the cold climate of China, *Energy Build.* 139 (2017 Mar) 371–384.
- [37] L. Callejas, L. Pereira, A. Reyes, P. Torres, B. Piderit, Optimization of natural lighting design for visual comfort in modular classrooms: Temuco case, *IOP Conf. Ser. Earth Environ. Sci.* 503 (1) (2020), 012007.
- [38] D. Salomón, S. Avalos Ambroggio, D. Salomón, S. Avalos Ambroggio, Optimization of classroom design: use of natural light for visual comfort in Villa María, Argentina, *Rev. Hábitat Sustentable.* 12 (1) (2022) 74–89.
- [39] F. Zhu, Y. Xu, Y. Jiang, Design optimization of daylighting for kindergarten in different light climate zones in China, *J. Asian Architect. Build. Eng.* 0 (0) (2023) 1–17.
- [40] Y. Liu, Y. He, Q. Deng, Form exploration of the top lighting system of educational buildings with setbacks based with multi-objective optimization, in: Proceedings of the National Conference on Architectural Digital Technology Teaching and Research, 2022, pp. 363–368. Available from: [https://kns.cnki.net/kcms2/article/abstract?v=3uoqIhG8C467SBI0vrai6TdxYisZCnOE4DdIn5fHra7whAmAecdzvaAkJDMe\\_bg5Ib7E14KQByPgzyJkXXkWNsxpNyee5ankIppgBnfaFs%3d&uniplatform=NZKPT](https://kns.cnki.net/kcms2/article/abstract?v=3uoqIhG8C467SBI0vrai6TdxYisZCnOE4DdIn5fHra7whAmAecdzvaAkJDMe_bg5Ib7E14KQByPgzyJkXXkWNsxpNyee5ankIppgBnfaFs%3d&uniplatform=NZKPT).
- [41] L. Wang, P. Janssen, K.W. Chen, Z. Tong, G. Ji, Subtractive building massing for performance-based architectural design exploration: a case study of daylighting optimization, *Sustainability* 11 (24) (2019) 6965.
- [42] L. Wang, H. Zhang, X. Liu, G. Ji, Exploring the synergy of building massing and façade design through evolutionary optimization, *Front. Architect. Res.* 11 (4) (2022) 761–780.
- [43] V. Katsanou, M. Alexiadis, D. Labridis, An ANN-based model for the prediction of internal lighting conditions and user actions in non-residential buildings, *J. Build. Perform. Simul.* 12 (5) (2019) 700–718.
- [44] R. da Fonseca, E. Didone, F. Pereira, Using artificial neural networks to predict the impact of daylighting on building final electric energy requirements, *Energy Build.* 61 (2013) 31–38.
- [45] C.L. Lorenz, A.B. Spaeth, C. Bleil de Souza, M.S. Packianather, Artificial Neural Networks for parametric daylight design, *Architect. Sci. Rev.* 63 (2) (2020) 210–221.
- [46] M. Arbab, M. Rahbar, M. Arbab, A comparative study of artificial intelligence models for predicting interior illuminance, *Appl. Artif. Intell.* 35 (2021), <https://doi.org/10.1080/08839514.2021.1882794>.
- [47] J. Ngarambe, I. Adilkhanova, B. Uwiragiye, G.Y. Yun, A review on the current usage of machine learning tools for daylighting design and control, *Build. Environ.* 223 (2022), 109507.
- [48] Y. Han, L. Shen, C. Sun, Developing a parametric morphable annual daylight prediction model with improved generalization capability for the early stages of office building design, *Build. Environ.* (2021) 200.
- [49] C.H. Lin, Y.S. Tsay, A metamodel based on intermediary features for daylight performance prediction of façade design, *Build. Environ.* 206 (2021), 108371.
- [50] L. Le-Thanh, H. Nguyen-Thi-Viet, J. Lee, H. Nguyen-Xuan, Machine learning-based real-time daylight analysis in buildings, *J. Build. Eng.* 52 (2022), 104374.
- [51] Y. Xu, C. Yan, H. Qian, L. Sun, G. Wang, Y. Jiang, A novel optimization method for conventional primary and secondary school classrooms in Southern China considering energy demand, thermal comfort and daylighting, *Sustainability* 13 (23) (2021 Dec).

- [52] M. Wang, S. Cao, D. Chen, G. Ji, Q. Ma, Y. Ren, Research on design framework of middle school teaching building based on performance optimization and prediction in the scheme design stage, *Buildings* 12 (11) (2022) 1897.
- [53] Y. Zou, Q. Zhan, K. Xiang, A comprehensive method for optimizing the design of a regular architectural space to improve building performance, *Energy Rep.* 7 (2021) 981–996.
- [54] A. Fora, *Designing the Sustainable school*, Images Publishing, 2007.
- [55] B. Piderit, M. Bodart, *Design Strategies Applied to Classroom's Daylight Design*, 2012, p. 6.
- [56] GB50099—2011, *Code for Design of School*, 2011 (in Chinese).
- [57] H. Pu, *Optimal Design of Natural Light Environment in Primary and Secondary School Classrooms in Guangzhou Based on Dynamic Daylighting Simulation*, South China University of Technology, 2021. Master, <https://kns.cnki.net/KCMS/detail/detail.aspx?dbcode=CMFD&dbname=CMFDTEMP&filename=1021894388.nh&v=>.
- [58] J. Ma, Q. Yang, Optimizing annual daylighting performance for atrium-based classrooms of primary and secondary schools in Nanjing, China, *Buildings* 13 (1) (2022) 11.
- [59] GB 55016-2021. *General Code for Building Environment* (in Chinese).
- [60] J. Snoek, H. Larochelle, R.P. Adams, Practical Bayesian optimization of machine learning algorithms, in: *Advances in Neural Information Processing Systems*, 2012, pp. 2951–2959.
- [61] *European Standard EN 17037*, Comité Européen de Normalisation, British Standard Institution, 2018.
- [62] P. Pilechiha, M. Mahdavejad, F. Pour Rahimian, P. Carnemolla, S. Seyedzadeh, Multi-objective optimisation framework for designing office windows: quality of view, daylight and energy efficiency, *J. Appl. Energy* 261 (2020), 114356, <https://doi.org/10.1016/j.apenergy.2019.114356>.